MANEUVERABILITY OF FULL BODIED SHIPS IN RESTRICTED WATERS

WITH SPECIAL REFERENCE TO THE COMPARISON
BETWEEN FULL SCALE DATA AND MODEL EXPERIMENT DATA

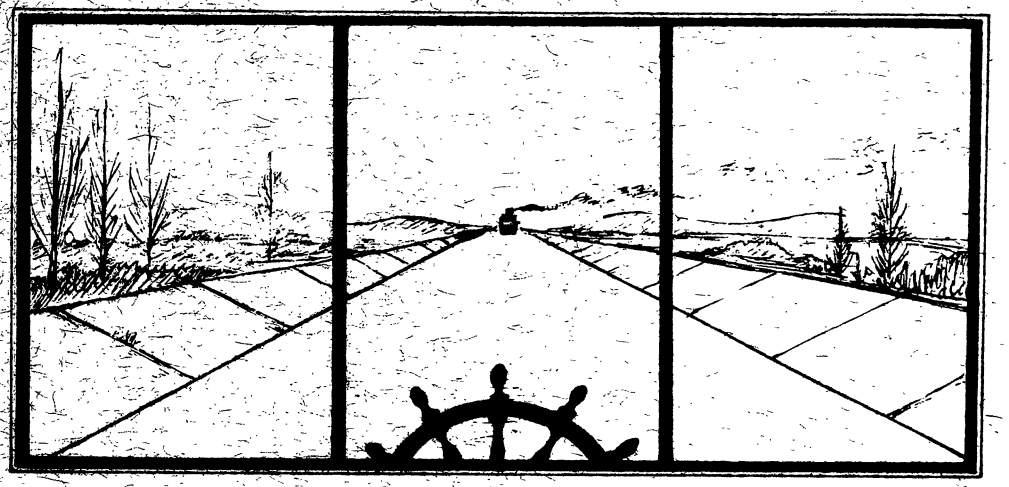

Department of Naval Architecture
and Marine Engineering
University of Michigan
450 West Engineering Building
Ann Arbor, Michigan

by

SEIZO MOTORA

and

RICHARD B. COUCH

Marine Technology

DEPARTMENT OF NAVAL ARCHITECTURE AND MARINE ENGINEERING

THE UNIVERSITY OF MICHIGAN

September 27, 1961

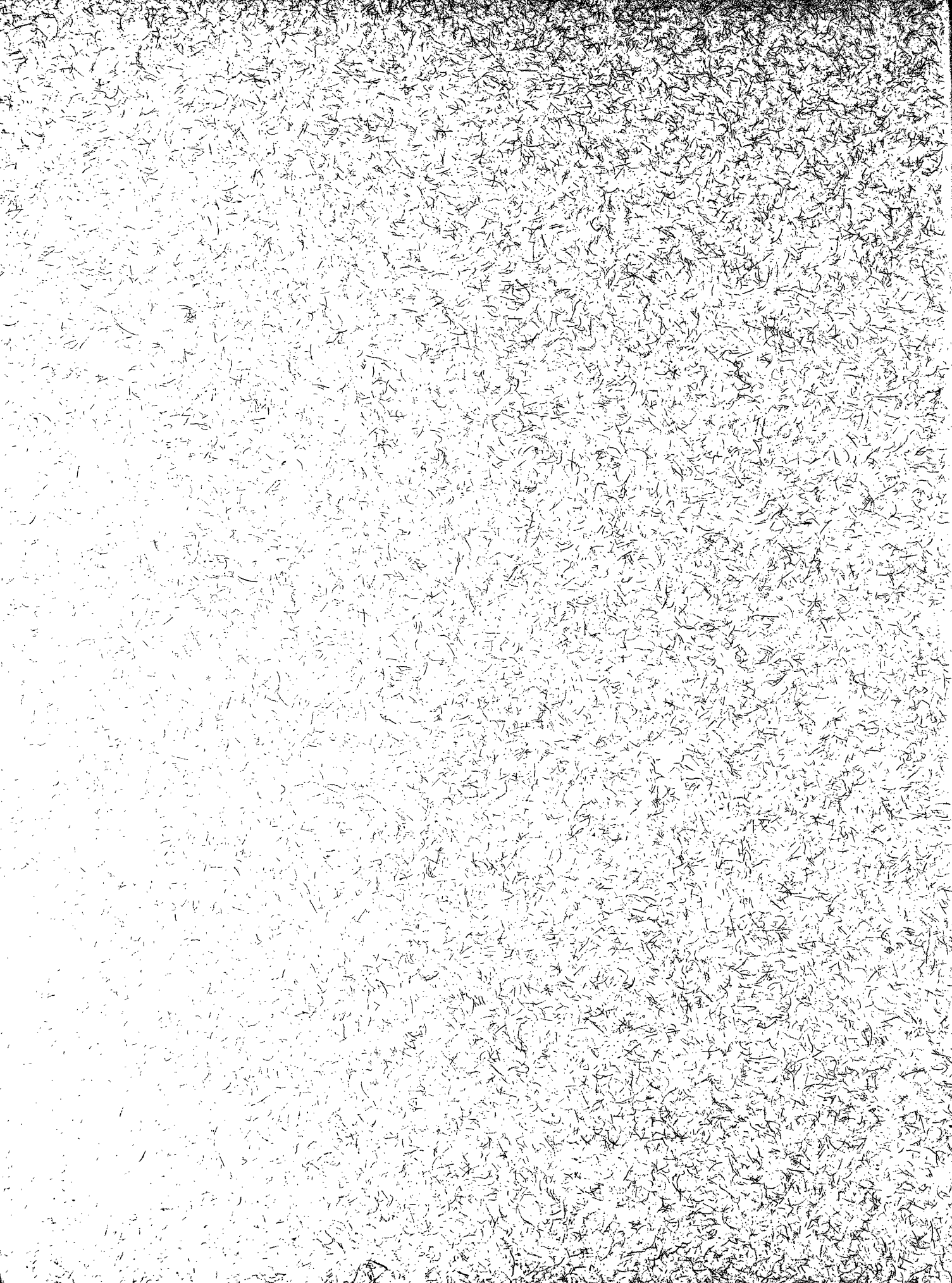

MANEUVERABILITY OF FULL BODIED SHIPS

IN RESTRICTED WATERS

With Special Reference to the Comparison Between Full Scale Data and Model Experiment Data.

by

Seizo Motora
Visiting Professor to The University of Michigan
from The University of Tokyo.

and

Richard B. Couch
Professor and Chairman of the Department of
Naval Architecture and Marine Engineering,
The University of Michigan.

Presented Before

The Fall Meeting of the Great Lakes and
Great Rivers Section
of
The Society of Naval Architects and
Marine Engineers.

Oct. 13th, 1961

CONTENTS, Continued

APPENDIX

1 EQUATION OF MOTION AND STABILITY DISCRIMINANT.....47

2 ANALYSIS OF FORCED YAWING TEST DATA.....52

3 CALCULATION OF THE RATE OF CHANGE OF COURSE VERSUS RUDDER ANGLE DIAGRAM.....54

LIST OF SYMBOLS

A	Lateral area
B	Breadth
D	Depth
d	Draft
G or C.G.	Center of gravity
I_z	Moment of inertia about z axis
J_z	Added moment of inertia about z axis
L l)	Length of the ship
m	Mass
m'	$m/\frac{1}{2}\rho l^3$
m_x	Longitudinal added mass
m_y	Transverse added mass
N	Moment about z axis
N'	$N/\frac{1}{2}\rho l^3 U^2$
$N(\dot{v})$	Moment about z axis due to $\dot{v}$
N(r)	Moment about z axis due to r
$N(\beta)$	Moment about z axis due to β
$N_{\dot{v}}$	$\partial N/\partial \dot{v}$
N_r	$\partial N/\partial r$
N_β	$\partial N/\partial \beta$
N'_r	$Nr/\frac{1}{2}\rho l^4 U$
N'_β	$N_\beta/\frac{1}{2}\rho l^3 U^2$
N'_δ	$N_\delta/\frac{1}{2}\rho l^3 U^2$
$N'_{\dot{r}}$	$N_{\dot{r}}/\frac{1}{2}\rho l^5$

continued

LIST OF SYMBOLS, Continued

O	Origin of co-ordinate
q_1, q_2, q_3	Coefficients of the characteristic equation
$r = \dot{\psi}$	Angular velocity about z axis
T	Period, Time constant, Maneuverability index
T_1, T_2, T_3	Roots of the characteristic equation
t	Time
t'	t x U/ℓ
U	Ship speed
u	x component of velocity
v	y component of velocity
x	x co-ordinate
Y	Side force
Y_v, Y_r ···	Derivatives
Y'	$Y/\frac{1}{2}\rho\ell^2U^2$
Y'_r	$Y_r/\frac{1}{2}\rho\ell^3U$
Y'_β	$Y_\beta/\frac{1}{2}\rho\ell^2U^2$
Y'_δ	$Y_\delta/\frac{1}{2}\rho\ell^2U^2$
y	y co-ordinate
z	z co-ordinate
α	Distance between C.G. and center of longitudinal added mass
β	Drift angle
δ	Rudder angle
ψ	Heading angle
ω	Circular frequency of yawing

INTRODUCTION

The need for the investigation of ship's maneuverability in shallow water and narrow channels such as in the Great Lakes area and in seaports has long been recognized; however, only limited full scale measurement or ship model studies have been performed for this purpose. In view of the importance of this problem, the Ship Hydrodynamics Laboratory of The University of Michigan is presently carrying out a wide range program of research in this field.

The initial full scale experiments were made on the Great Lakes ore carrier S.S. BENJAMIN FAIRLESS followed by model experiments on a model of the same ship by means of a forced yawing technique. The comparison of the results from these tests showed a reasonable agreement; therefore, the authors were encouraged to carry out additional model experiments in shallow water and in narrow channels. Because it is impractical to carry out full scale tests in narrow channels, we hope that the results from these model experiments will be of value.

In this paper we have given descriptions of the full scale tests and the model experiments followed by an evaluation of the accuracy and reliability of the forced yawing technique.

Further information concerning the analysis of restricted water effects will be reported at a later date.

CHAPTER 1

TYPES OF FULL SCALE MANEUVERING TESTS EMPLOYED

The following test techniques were used to obtain information about the maneuverability of a full scale ship.

1.1 Spiral Test

This test was initiated by Deudonné (1) for evaluating the directional stability of ships. The test is performed in the following manner; the ship is first set on a straight course, then the rudder is turned to the right to a specified angle. When the ship attains a stationary turn, the rudder angle is reduced by a small angle and kept in this position until the ship again attains a stationary turn. The rudder angle is changed step by step in this manner until a certain left rudder angle is obtained. The same procedure is repeated starting with a specified left rudder angle. The heading angle and the rudder angle are measured at given time intervals during the complete test, and the rate of change of heading of the ship can be computed from these results and plotted versus the rudder angle.

This plot obtained from the spiral test can be of two different types, depending on the directional stability of the ship. If the ship is directionally stable, the diagram will be of the form shown in Fig. 1.a. It is seen from the plot that the ship has only one turning rate for a given rudder angle, and that the direction of turning is always the same as the rudder angle. On the other hand, if the diagram is as given in Fig. 1.b, the

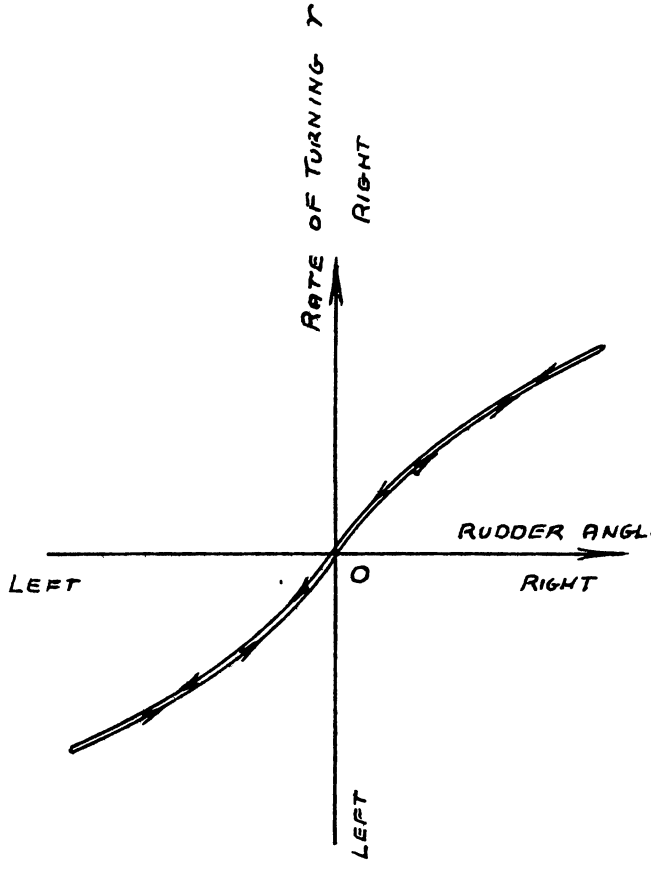

FIG. 1. a

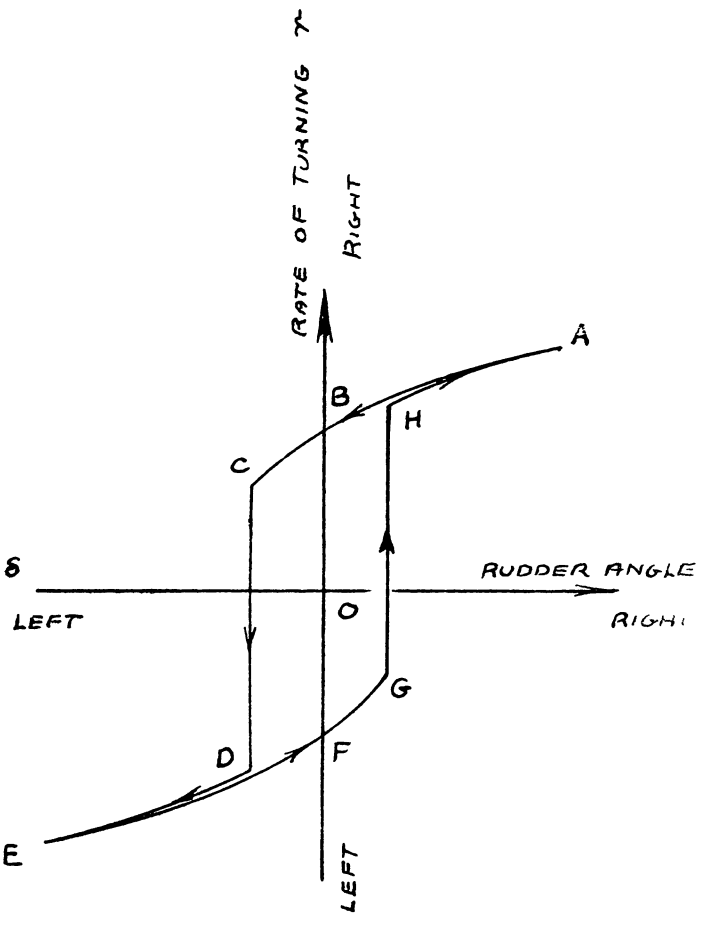

FIG. 1. b

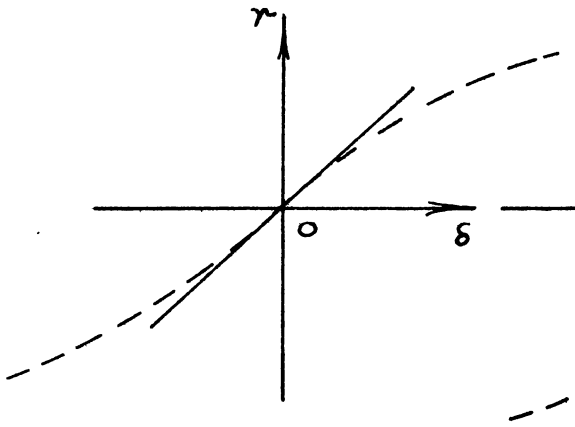

FIG. 2. a

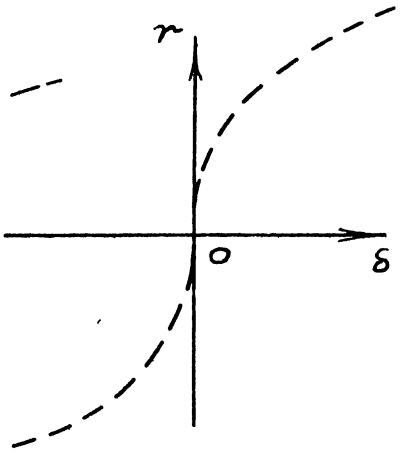

FIG. 2. b

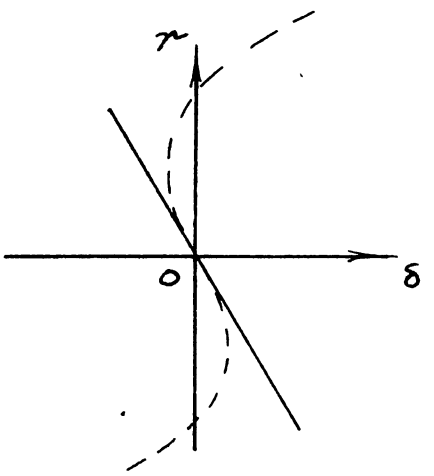

FIG. 2. C

ship is said to be directionally unstable. This diagram shows that when the rudder angle is reduced from A to B (at B, rudder angle is zero) the ship still has a certain amount of turning rate at B, and will therefore continue to turn to the right even after the rudder is turned to the left. When the rudder is put as far to the left as point C, the ship will suddenly reverse its direction of turn. The jump from point C to D on the diagram indicates this. The same phenomenon will occur when the rudder angle is changed from point E towards F, and the ship will turn against the rudder from F to G and then reverse the direction of turn at G. This shows that the ship has two different ways of turning for the same rudder angle depending on the initial conditions.

This phenomenon can be explained somewhat theoretically as follows: In Appendix I it is shown that the turning rate versus rudder angle diagram at zero rudder angle, $\left(\frac{\partial r}{\partial \delta}\right)_{at\ \delta=o}$ has a special correlation with the directional stability of the ship; if a ship is directionally stable, then the angle of the tangent is positive as shown in Fig. 2.a; if a ship has neutral stability, the angle of the tangent is vertical as in Fig. 2.b; and if a ship is unstable, the angle of the tangent is negative as in Fig. 2.c. When assuming that the hydrodynamic forces and moments acting on the ship are linear, the diagram of the turning rate versus the rudder angle should be a straight line which coincides with the tangent at the origin. In such an assumed case

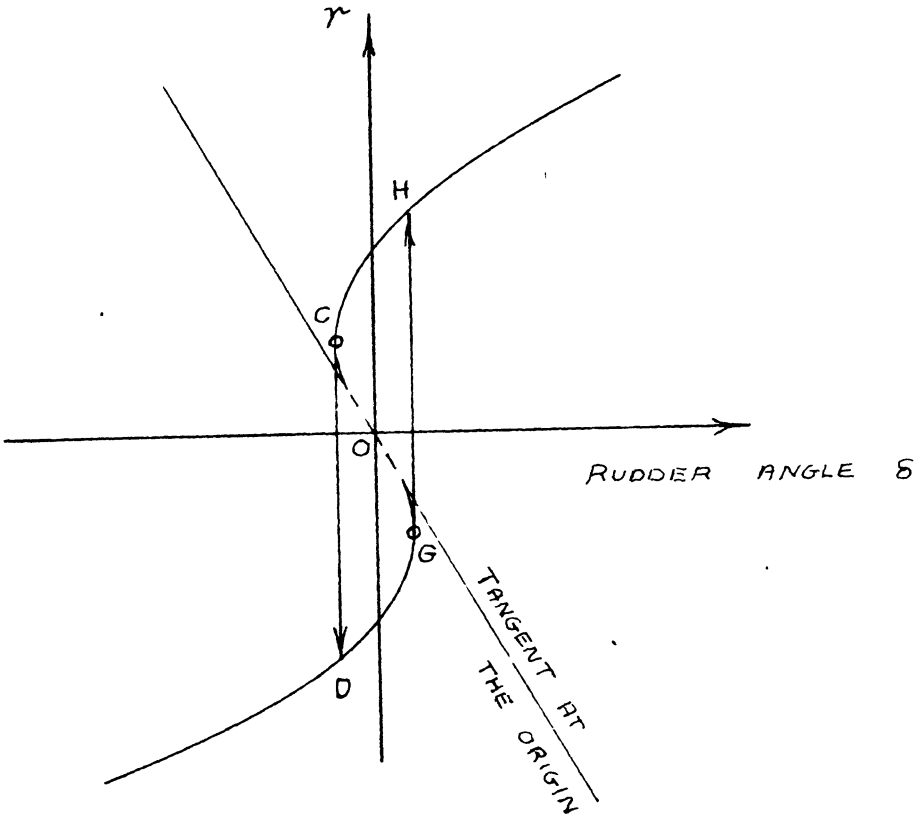
r
H
C
O
RUDDER ANGLE δ
G
TANGENT AT THE ORIGIN
D

FIG. 3

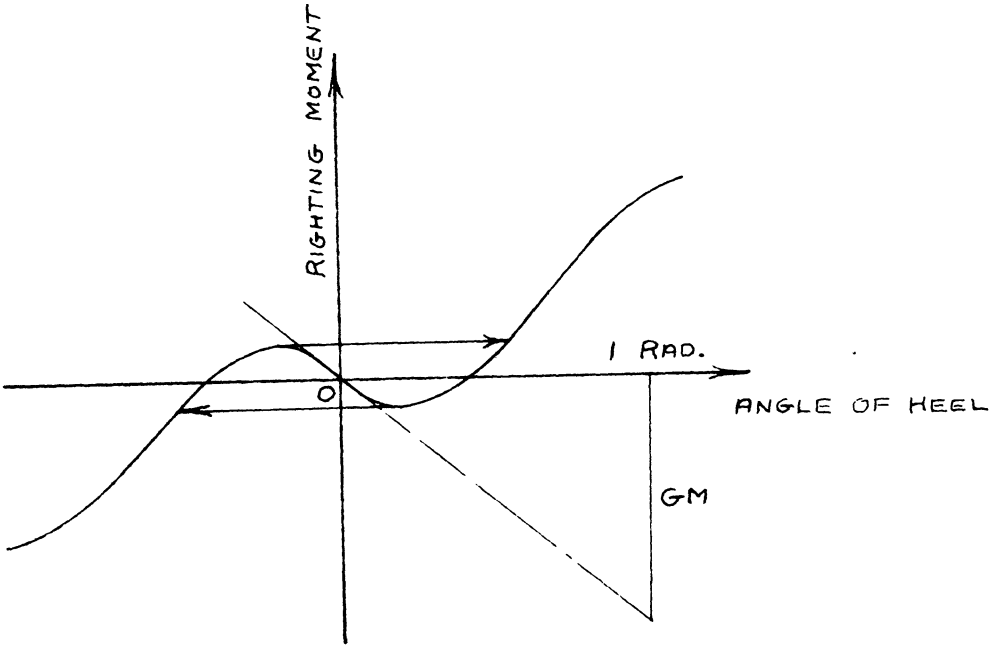
RIGHTING MOMENT
1 RAD.
O
ANGLE OF HEEL
GM

FIG. 4

no stationary turn exists in the direction of the rudder angle when a ship is directionally unstable, as seen in Fig. 2.c. In actual cases the diagrams will be as indicated by the broken lines in Fig. 2, because the hydrodynamic forces and moments are non-linear.

Fig. 3 is an enlarged view of Fig. 2.c. Between point C and G there exists, theoretically, an infinite number of solutions which satisfy the equations of motion (A·8); however, these solutions have been proved to be in unstable equilibrium (2) in actual cases. There will therefore be jumps in the diagram from C to D and from G to H and these jumps will form a hysteresis loop in the diagram for an actual test as shown in Fig. 1.b. It should be noticed that the more unstable the ship, in other words the less steep the tangent at the origin, the larger the size of the loop.

This phenomenon is quite similar to the case of the equilibrium of a ship which has a negative GM. The similarity can be seen from Fig. 4.

1.2 Zig-Zag Test (Serpentine Test)

This test was initiated by Kempf (3) to obtain general information on maneuverability. The test is performed in the following manner: The ship is first set on a straight course, then the rudder is turned to a predetermined angle (say 20° right). When the heading angle of the ship has changed the same amount as the rudder angle (20° right), the rudder is immediately reversed to the opposite side (20° left) and kept constant. As

soon as the heading angle attains the same angle as the rudder angle (20° left), the rudder is again reversed (to 20° right). This cycle is repeated about twice.

During this test the heading angle and the rudder angle are recorded and plotted versus the time elapsed as shown in Fig. 5. One of the measures of maneuverability is the total distance run to complete the test. According to Kempf (3), the total distance run of a ship which has adequate maneuverability should lie between 6 to 10 times the length of the ship. A distribution diagram of the total distance run given by Kempf is shown in Fig. 6.

The overshoot angle (see Fig. 5) is another measure of the maneuverability and the larger the overshoot angle the less stable the ship.

It has been shown by Nomoto (4) that the maneuverability of a ship can be expressed analytically by two indices, and that these two indices can be obtained analytically from the zig-zag test data. The one index K represents the turning ability and the other index T the quickness of response. Physical meaning of these indices will be explained as follows: If we plot the change of heading angle (ψ) due to steering versus the time elapsed, the curve will have the form shown in Fig. 7. This curve can in general be simulated by a simple exponential curve:

$$\psi = K\delta \cdot T + K\delta\left(1 - e^{-\frac{t}{T}}\right)$$

where ψ = heading angle
δ = rudder angle
t = time

$$\psi = -K\delta T + K\delta t + K\delta T\left(e^{-t/T}\right)$$

$$= K\delta T\left(\frac{t}{T} + e^{-\frac{t}{T}} - 1\right) \approx K\delta T\left(\frac{\left(\frac{t}{T}\right)^2}{2} - \frac{\left(\frac{t}{T}\right)^3}{6} + \cdots\right) \quad t \to 0$$

$$\approx K\delta(t - T) \quad t \to \infty$$

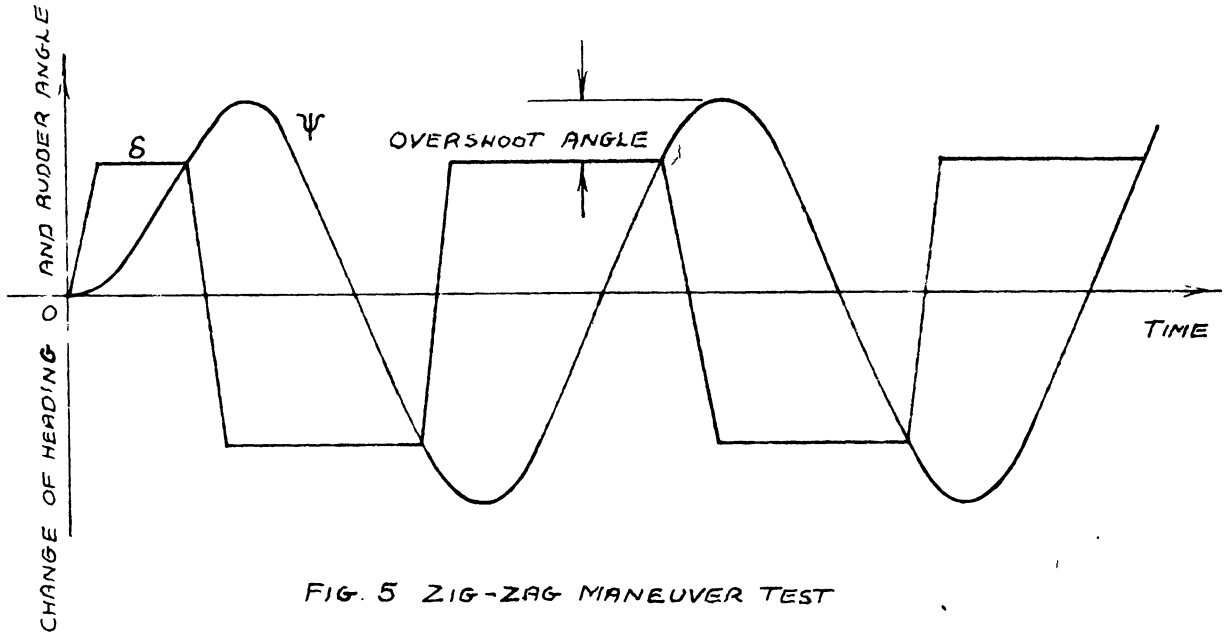

FIG. 5 ZIG-ZAG MANEUVER TEST

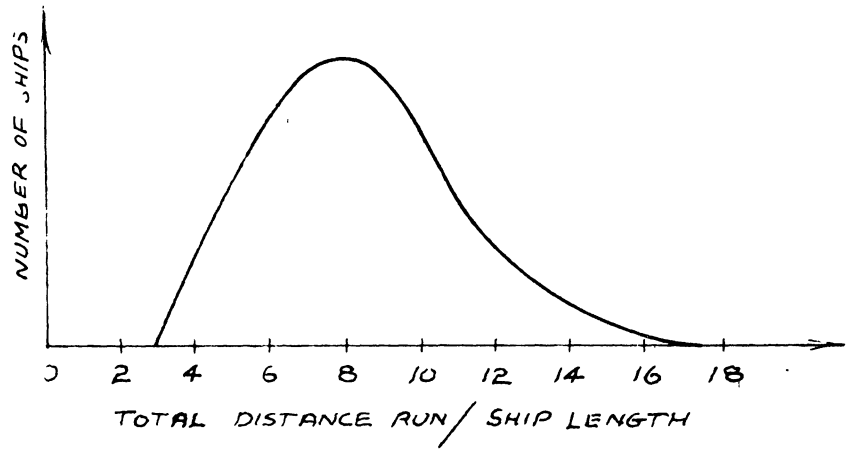

FIG. 6

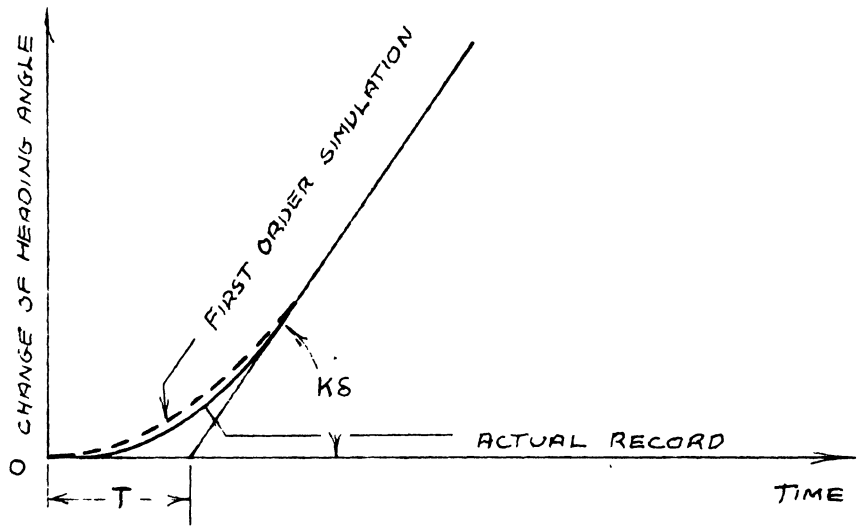

FIG. 7

Therefore it follows that T is the time lag to reach a stationary turn, and that K times δ is the slope of the curve at stationary condition. The larger the T, the more sluggish the response to the rudder, and the larger the K, the better the turning ability of the ship. It can also be easily verified that T has a close relationship to the directional stability and the larger the T the less stable the ship (4).

1.3 Continuous Recording of Heading Angle and Rudder Angle

This test gives correlations between the rudder angle as an input and the heading angle as an output when considering the ship as an open loop servo system. This test is suitable for restricted areas where spiral or zig-zag tests are not practicable.

CHAPTER 2

FULL SCALE MANEUVERING TESTS ON S.S."BENJAMIN FAIRLESS"

2.1 Description of the Ship and Test Conditions

The Great Lakes ore carrier S.S. BENJAMIN FAIRLESS was provided as a representative ship by the Pittsburgh Steamship Division of United States Steel Corp. Tests were conducted on two occasions, the first in October 1960 on the Detroit River and Lake Erie, and the second in July 1961 on Lake Michigan.

The dimensions of the ship are given in Table 1, while types of tests, location of the testing area, and the conditions of the ship are given in Table 2. The right hand column in Table 2 indicates in which figure the results of each test are shown.

Following are short descriptions and discussions of the results shown in Figs. 8 to 15.

Fig. 8 Spiral test in shallow water.

Stationary turning rate in degrees per second is plotted versus the rudder angle in degrees. The hysteresis loop is fairly large which indicates that the ship has a typical tendency toward instability. Plots A and C in Fig. 8 are believed to be of the shape given in plots B and D if measurements were continued until motion became stationary.

Fig. 9 20°-20° Zig-zag test in shallow water.

The heading angle in degrees and the rudder angle in degrees are plotted versus the elapsed time in minutes.

TABLE 1

SHIP DIMENSIONS

LOA	639' 6"
LBP	622' 9"
LWL	621' 7"
Breadth molded	67' 0"
Depth molded	35' 0"
d_{max}	24' 0"
Deadweight	18,000 L.T.
Gross Tonnage	10,450
Displacement	23,960 L.T. 24343.4 T
SHP normal	4,000
SHP max	4,400
RPM normal	90
RPM max	93
Rudder size	10' 8" x 22' 1½"
Propeller:	
Diameter	17' 6"
Pitch	14'9.7"
Area	109.5 sq. ft.
Blades	4
Rake	6 3/4"

TABLE 2a

FIRST FULL SCALE TRIALS

(d_f=21 feet, d_a=23 feet)

Test No.	1	2	3	4	5	6
Type of Test	Spiral test in shallow water	20^o-20^o zig-zag test in shallow water	20^o-20^o zig-zag test in medium depth	20^o-20^o zig-zag test in deep water	10^o-10^o zig-zag test in deep water	30^o-30^o zig-zag test in deep water
Time	7:30-8:00 PM	8:20-8:40 PM	7:00-7:20 AM	8:50-9:10 AM	7:40-8:40 AM	8:20-8:40 AM
Date, 1960	Oct. 4	Oct. 4	Oct. 5	Oct. 5	Oct. 5	Oct. 5
Position	5 miles N. of Middle Sister Is.	same ←	330^o, 5 miles off Conneaut, Ohio	320^o, 5 miles off Conneaut, Ohio	325^o, 10 miles off Conneaut, Ohio	320^o, 15 miles off Conneaut, Ohio
Depth of Water	30 ft.	30 ft.	36-48 ft.	72 ft.	48-60 ft.	72 ft.
RPM	84	84	88	84	86	83
MPH	13	13	13.6	13	13.5	13.2
Figure	8	9	10	11	-	-

TABLE 2b

SECOND FULL SCALE TRIALS

(d_f=23 feet, d_a=23 feet 6 inches)

Test No.	7	8,9	10	11
Type of Test	Continuous recording in channel	Spiral test in deep water	20°-20° zig-zag test in deep water	Continuous recording in deep water
Time Date, 1961	7:00-7:30 PM June 29	10:20-11:40 AM June 30	11:50 AM-12:10 PM June 30	12:20-12:50 PM June 30
Position	#4 channel down the Soo	308°, 24 miles off Pt. Betsie, Lake Mich.	same ←	same ←
Depth of Water	27 ft.	300 ft.	same ←	same ←
RPM	70	94	94	94
MPH	10	14.2	14.2	14.2
Figure	12	13	14	15

The data should be compared with the data from the deep water test, Figs. 11 and 14.

Fig. 10. Zig-zag test in medium depth water.

The wind was strong and the depth of water varied from 36 feet to 48 feet; therefore this datum gives only rough information.

Fig. 11 20°-20° zig-zag test in deep water.

The wind was somewhat strong during this test and this might have had some effect on the results.

Fig. 12 Continuous measurement of the helm angle and the heading angle in the channel.

Records were taken over 30 minutes, but records over only 3 minutes are shown as an example. Excessive right rudder should be noted. This might have been caused partly by the right hand rotation of the propeller, and partly by the off-center position of the ship in the channel.

Fig. 13 Spiral test in deep water.

This test was conducted over a longer period so that the ship would attain a stationary motion. These data should be quite reliable because wind was light and the surface was calm during this test. Shallow water results are added for comparison.

Fig. 14 20°-20° zig-zag test.

These data are also thought to be quite reliable.

Fig. 15 Continuous record of helm angle and heading angle.

Excessive right rudder should be noted.

2.2 Analysis of Data

2.2.1 Analysis of spiral tests.

From Fig. 8 and Fig. 13, it is seen that the ship has a typical tendency toward instability both in deep and in shallow water, and comparing Fig. 8 and Fig. 13, it is noted that the effect of shallow water is to make a ship more nearly stable than in deep water.

For comparison with other ships, height and width of the hysteresis loops are measured and plotted in Fig. 16 and Fig. 17 together with data from Gertler and Gover (5). From Fig. 16 and Fig. 17, it can be seen that the ship is quite unstable in deep water and fairly unstable in shallow water in comparison with the general average of other ships.

2.2.2 Analysis of zig-zag test.

Remarkable differences, especially in overshoot angle will be noticed when comparing shallow water test data (Fig. 9) to deep water tests data (Figs. 11 and 14). In Fig. 18, the overshoot angle for each test is plotted and compared with data from Gertler and Gover (5). In Fig. 18, the remarkable change in the overshoot angle due to the change of water depth should be noticed.

Maneuverability indices T and K are also calculated from the data and shown in mon-dimensional form ($T' = T \times U/\ell$ and $K' = K \times \ell/U$) in Fig. 19. The base of Fig. 19 is $1/T'$ which is proportional to the quickness of response, and the ordinate is

$1/K'$ which is proportional to the inverse of turning ability; therefore, the right side of Fig. 19 indicates quicker response and the lower part of Fig. 19 indicates better turning ability. From Fig. 19, it can be seen that the ship is more responsive to the rudder but less turnable in shallow water than in deep water.

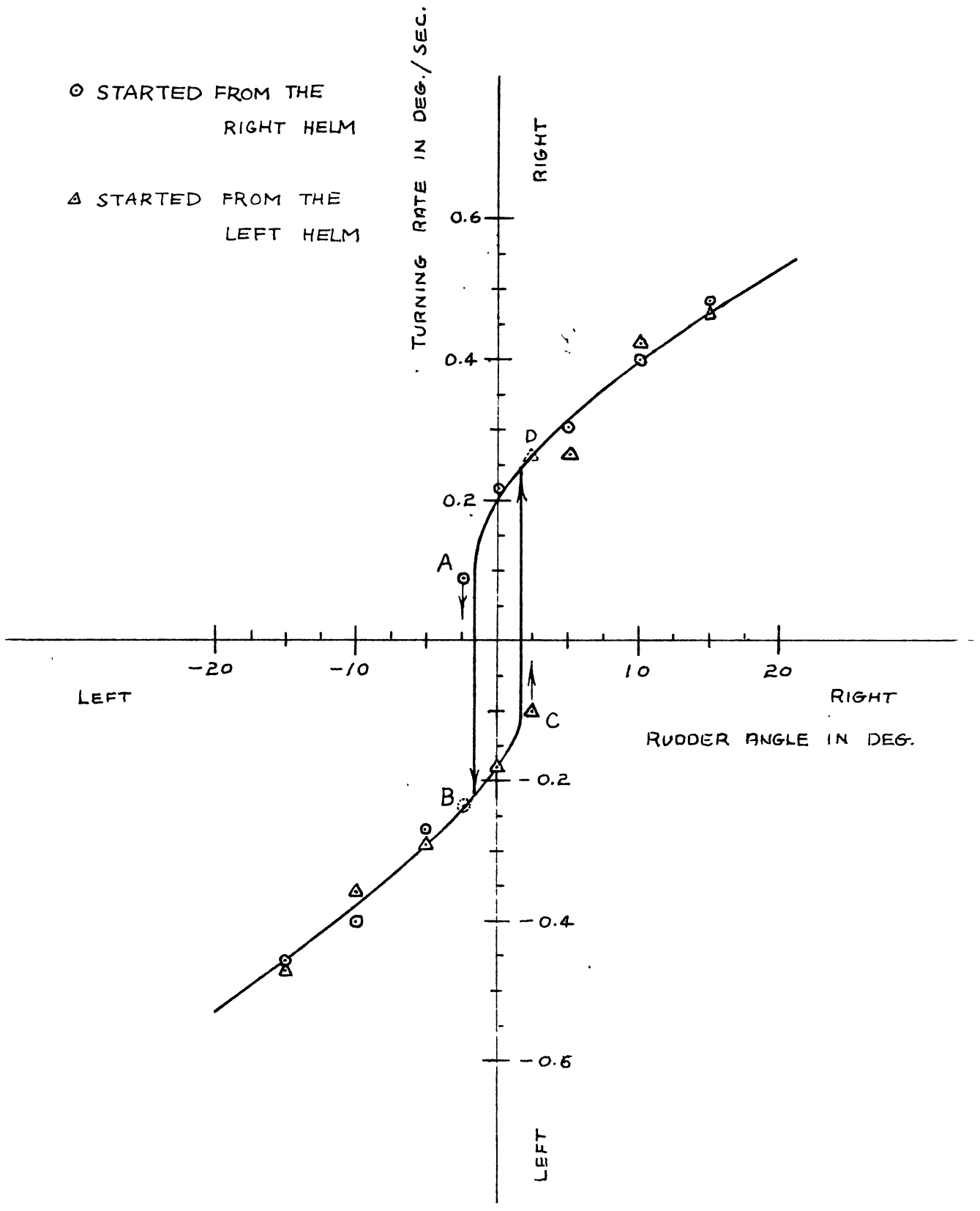

FIG. 8 SPIRAL TEST IN SHALLOW WATER

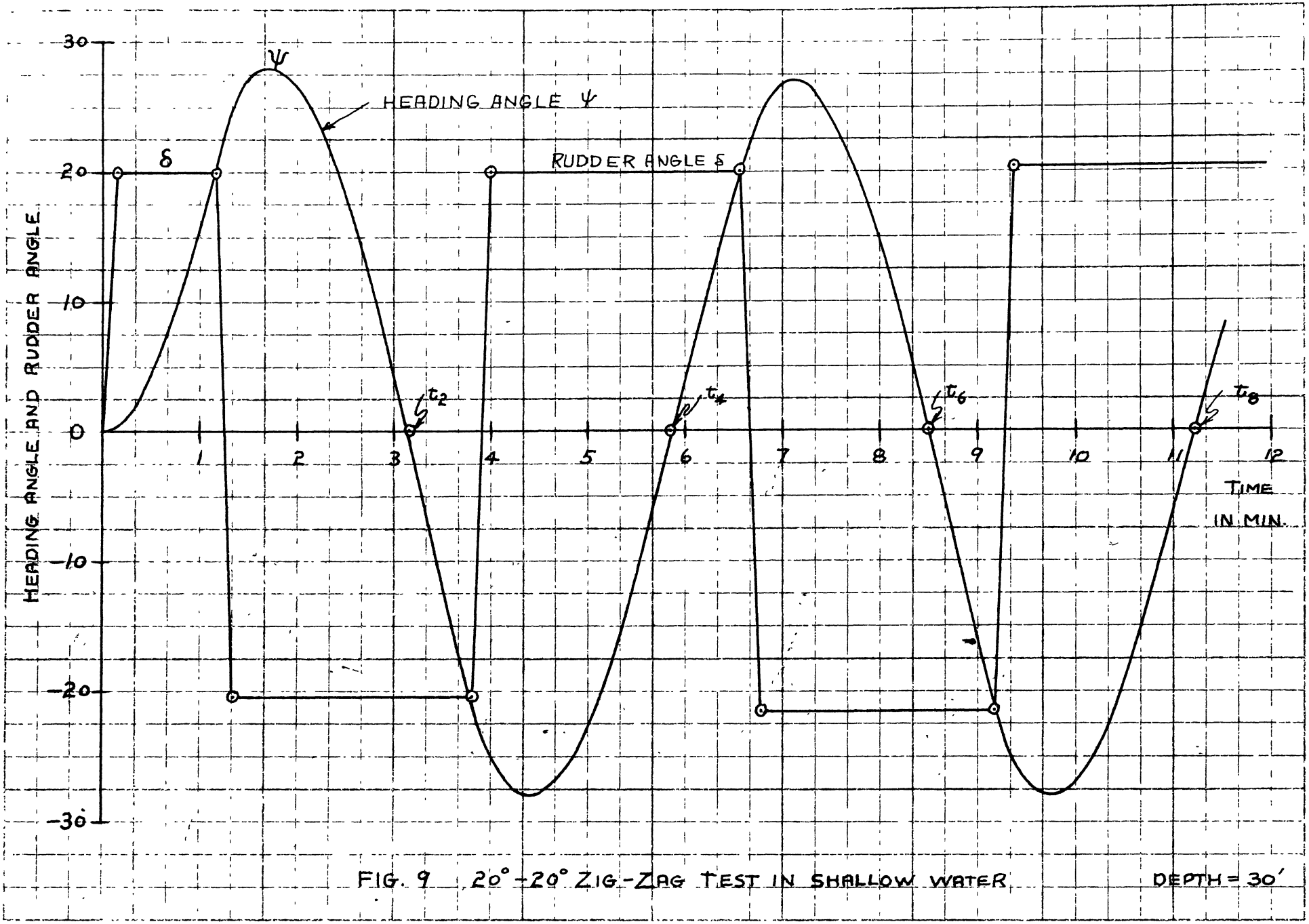

FIG. 9 20°-20° ZIG-ZAG TEST IN SHALLOW WATER DEPTH = 30'

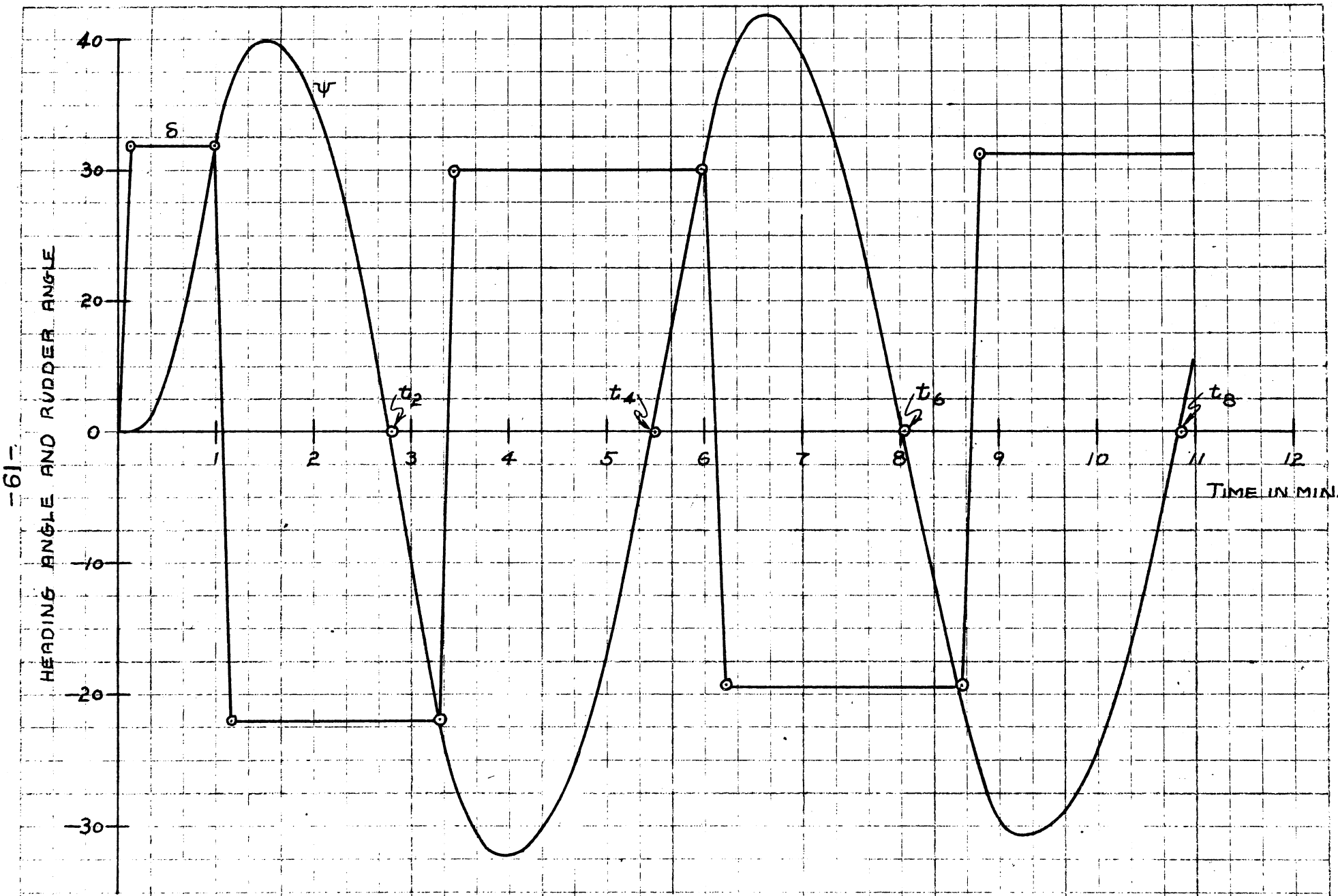

FIG. 10 20°–20° ZIG-ZAG TES[illegible] DEPTH (IND.3) DEPTH = 45'

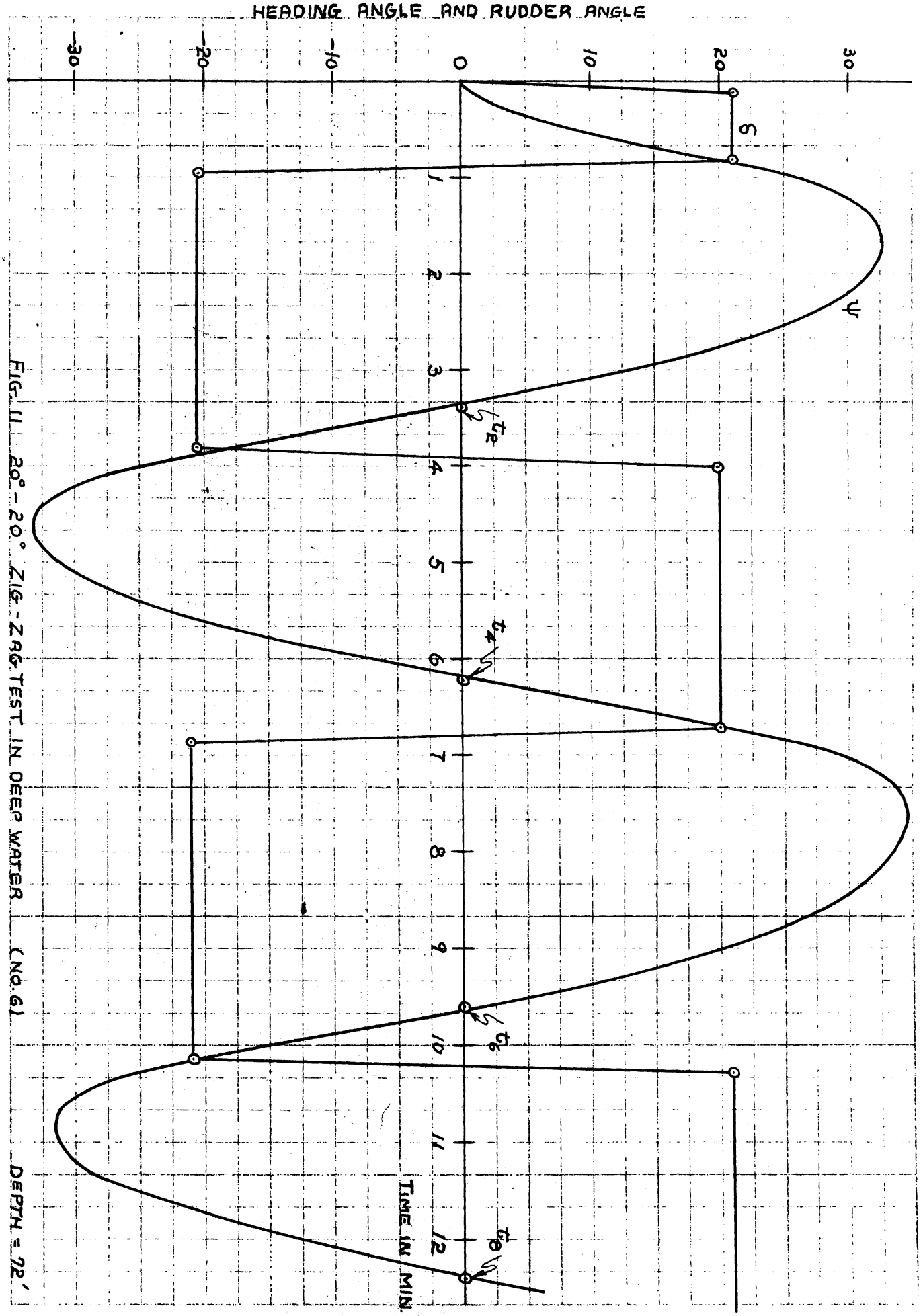

FIG. 11 20°-20° ZIG-ZAG TEST IN DEEP WATER (NO. 6). DEPTH = 22'

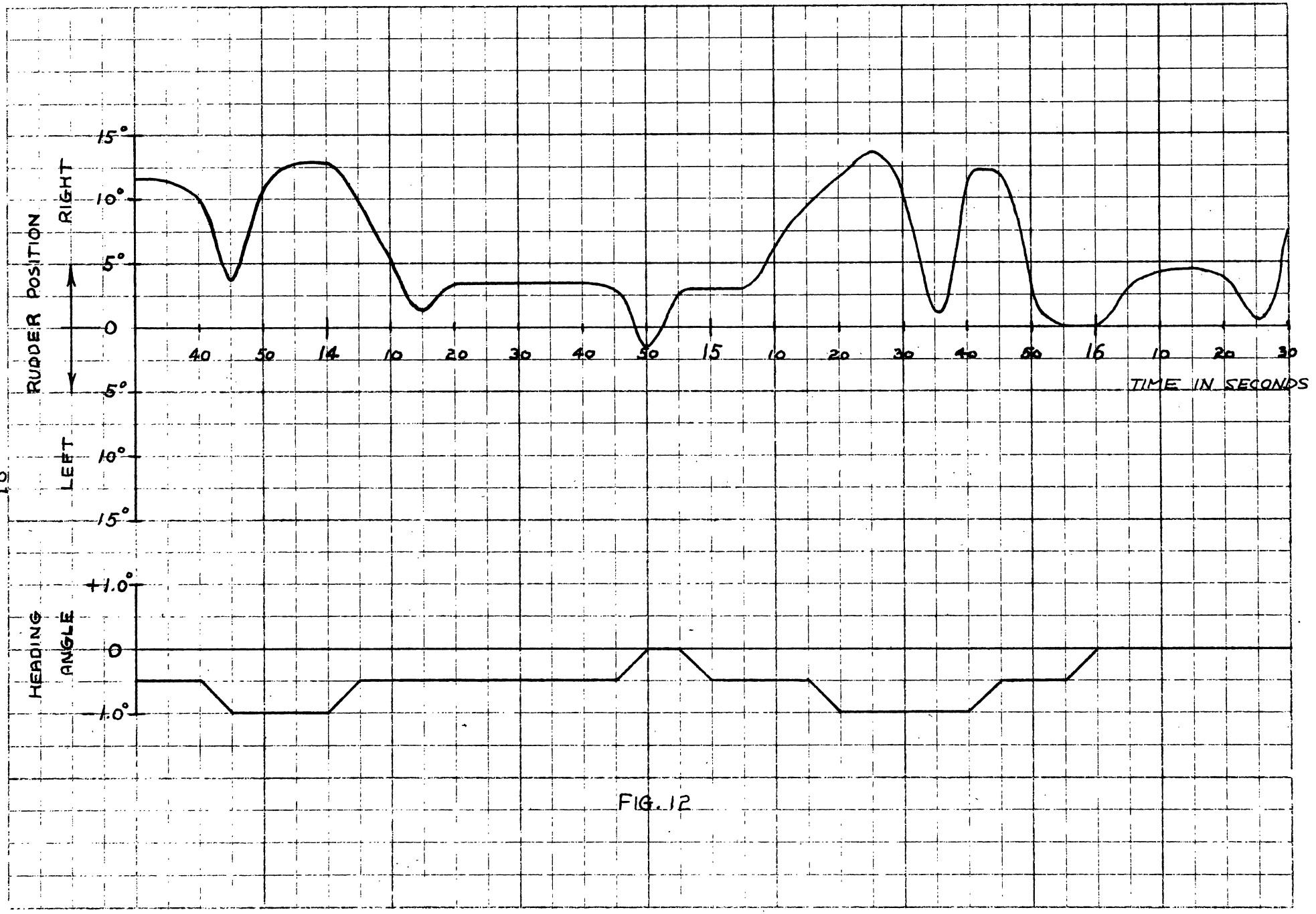

FIG. 12

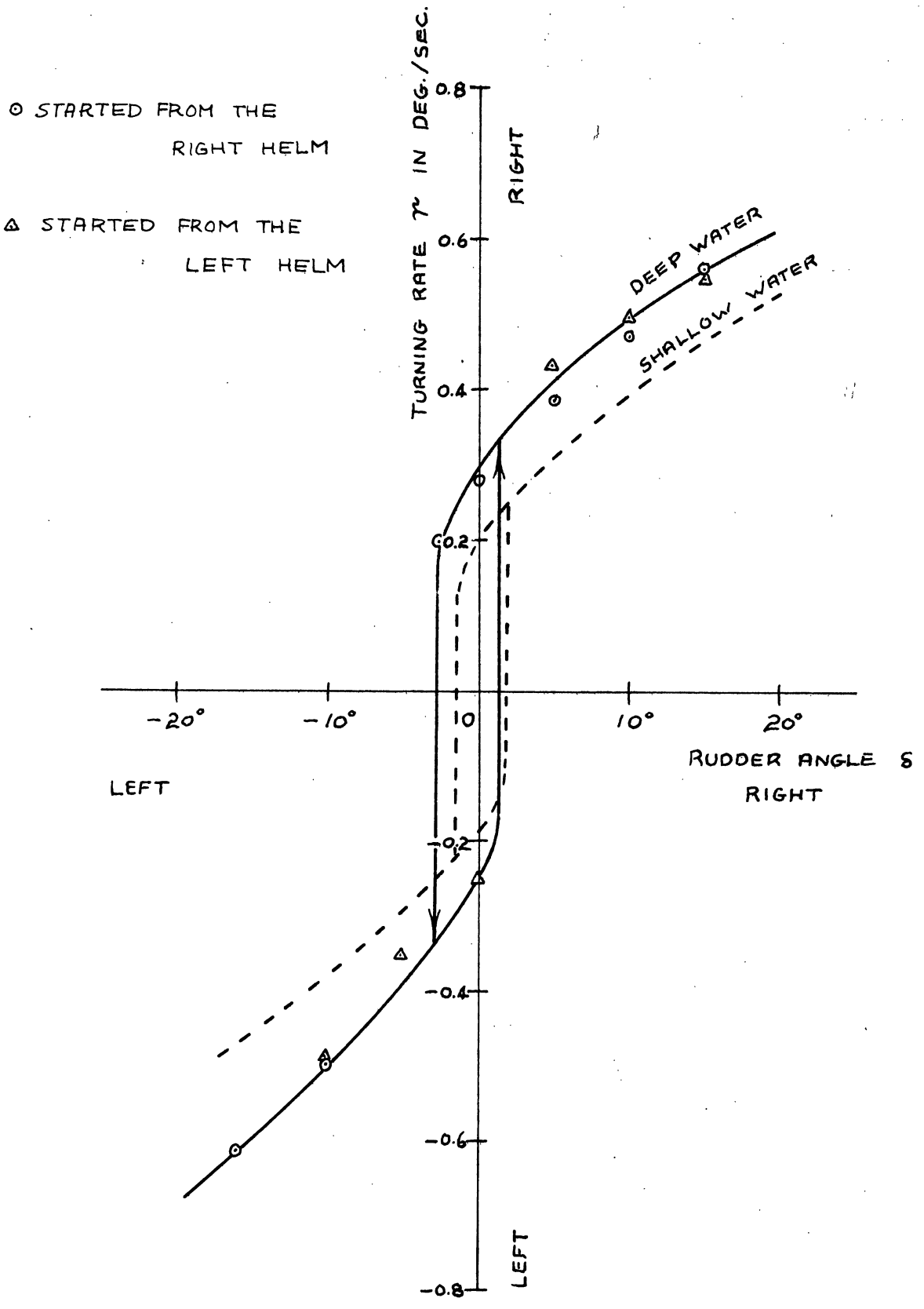

FIG. 13 SPIRAL TEST IN DEEP WATER

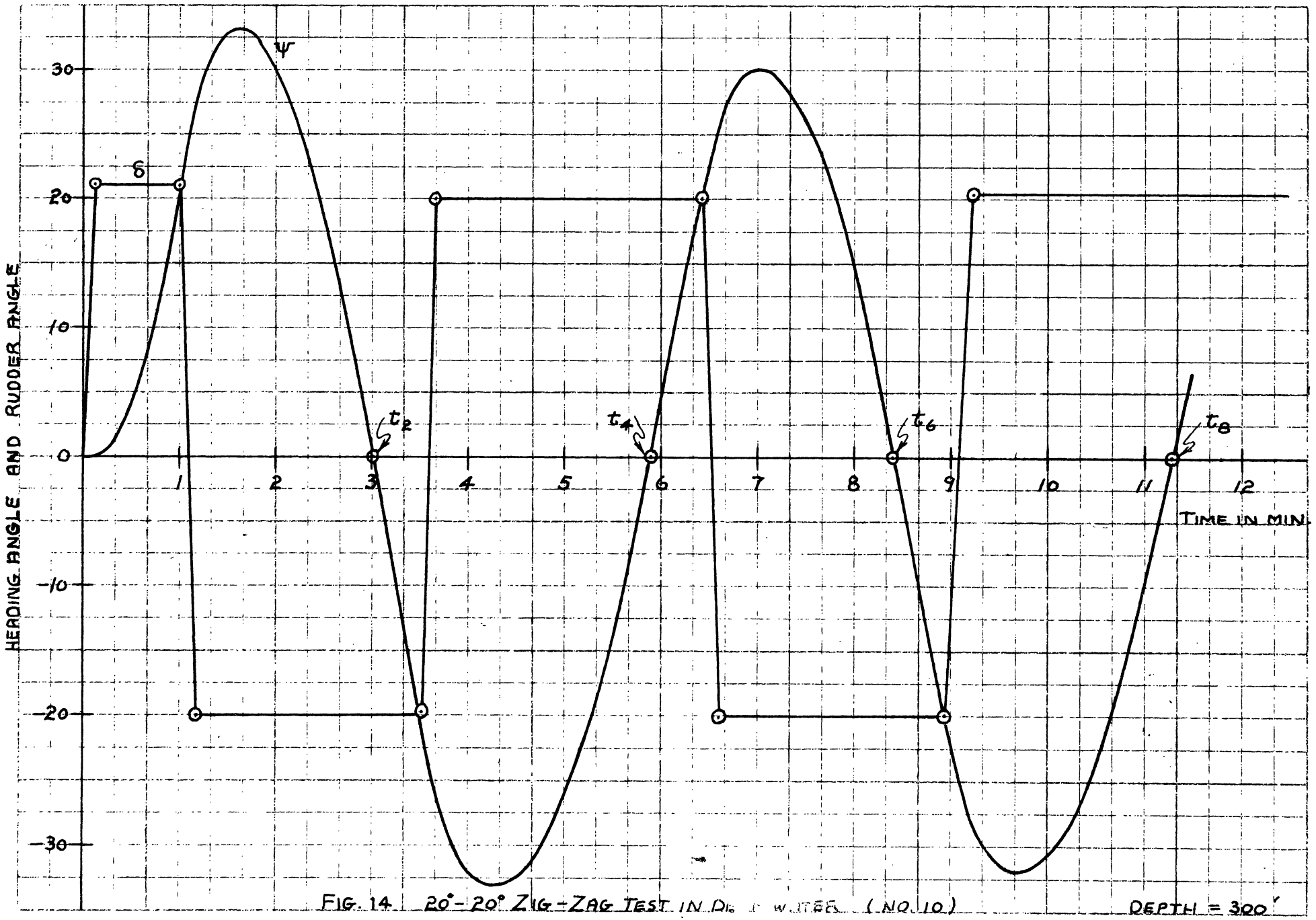

FIG. 14 20°-20° ZIG-ZAG TEST IN DEEP WATER (NO. 10) DEPTH = 300'

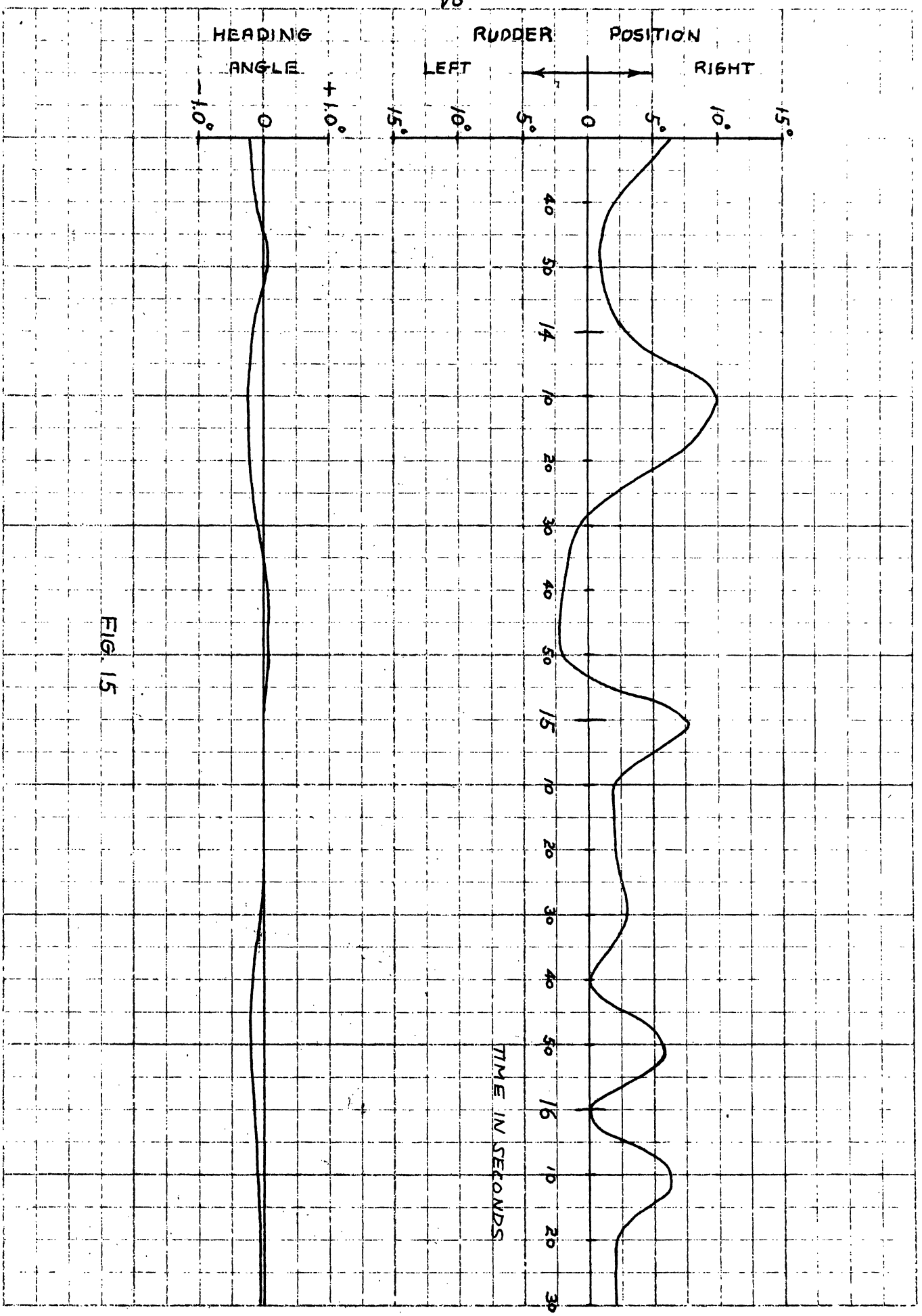
HEADING ANGLE
-1.0°
0
+1.0°
RUDDER POSITION
LEFT
RIGHT
15°
10°
5°
0
5°
10°
15°
40
50
1/4
10
20
30
40
50
1/5
10
20
30
40
50
1/6
10
20
30
TIME IN SECONDS

FIG. 15

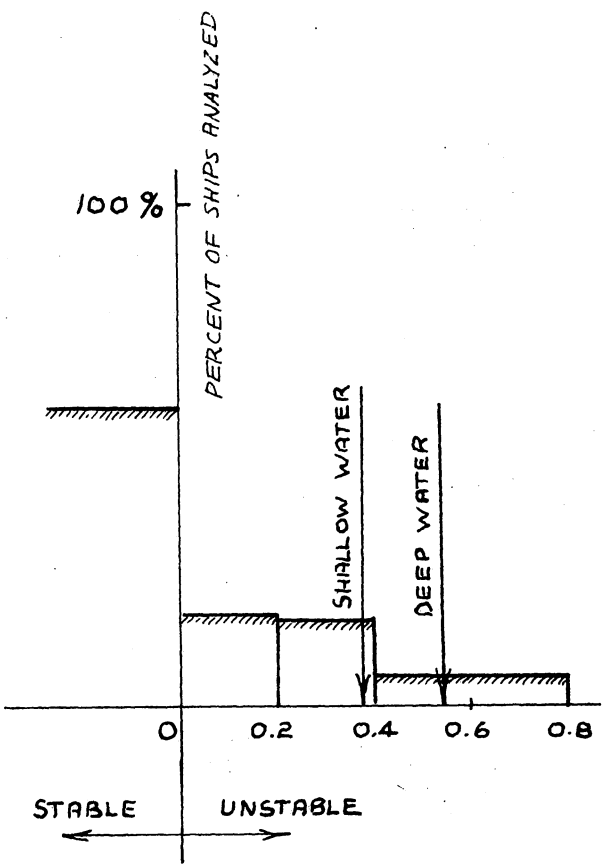

HEIGHT OF LOOP

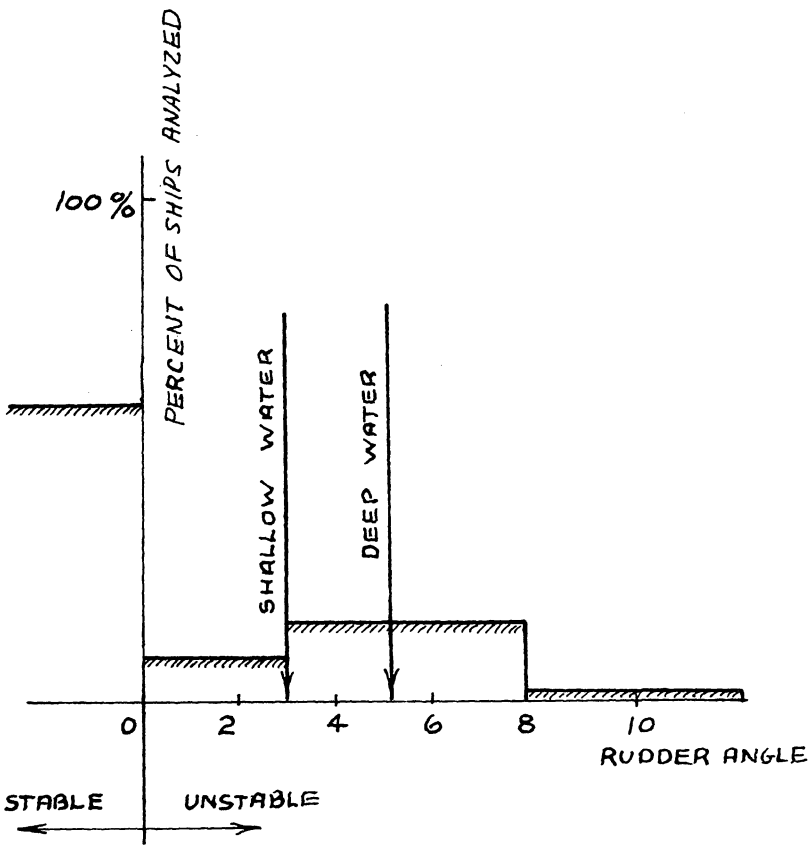

WIDTH OF LOOP

FIG. 16

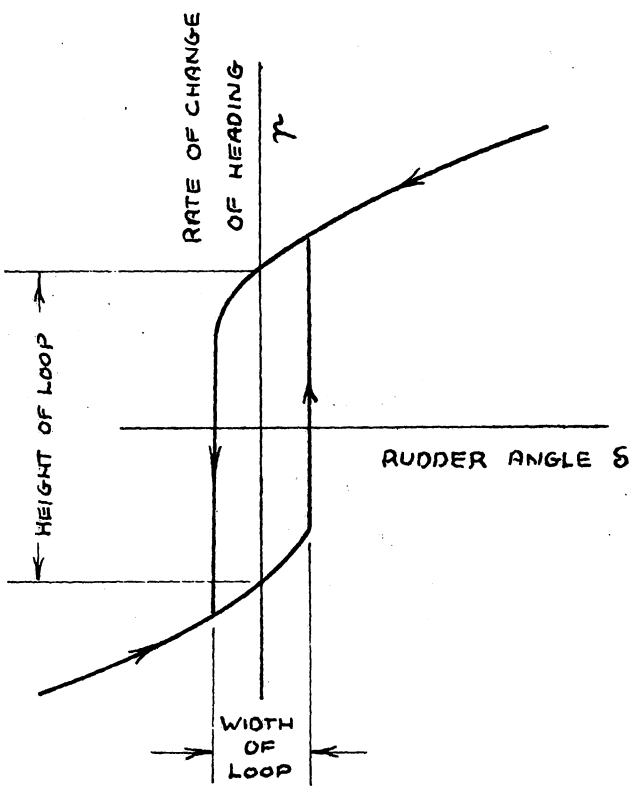

FIG. 17

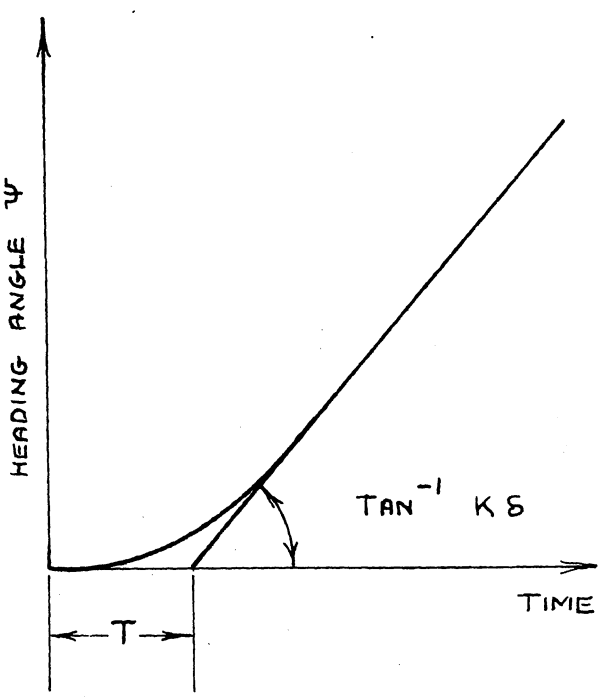

FIG. 18

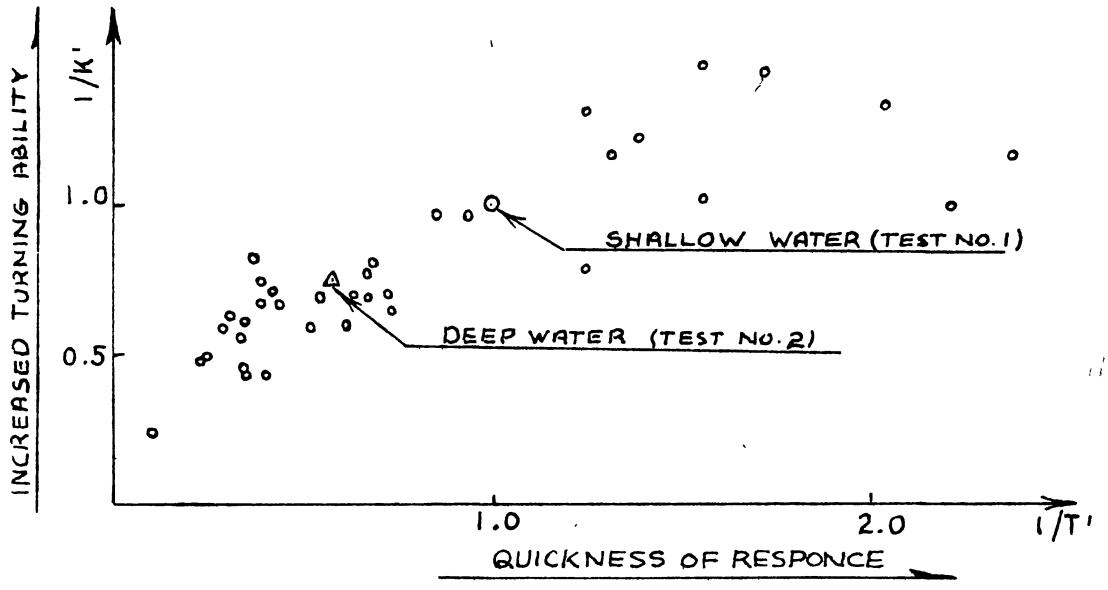

FIG. 19 MANEUVERABILITY INDICES

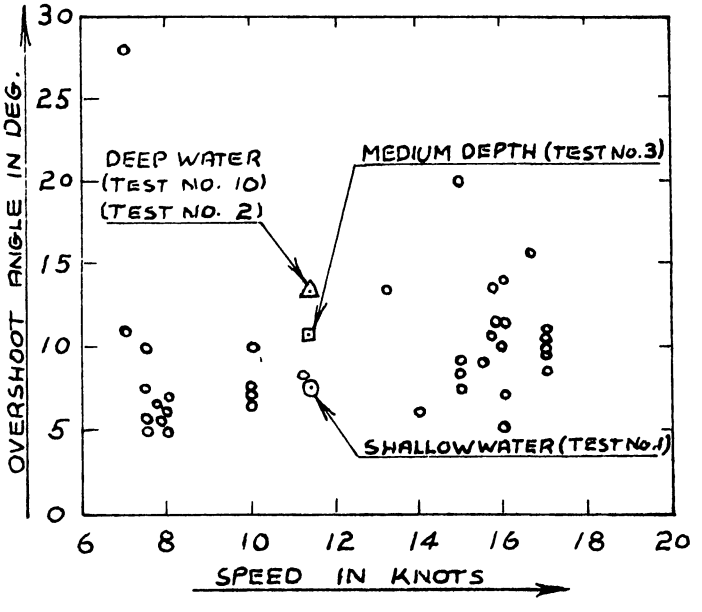

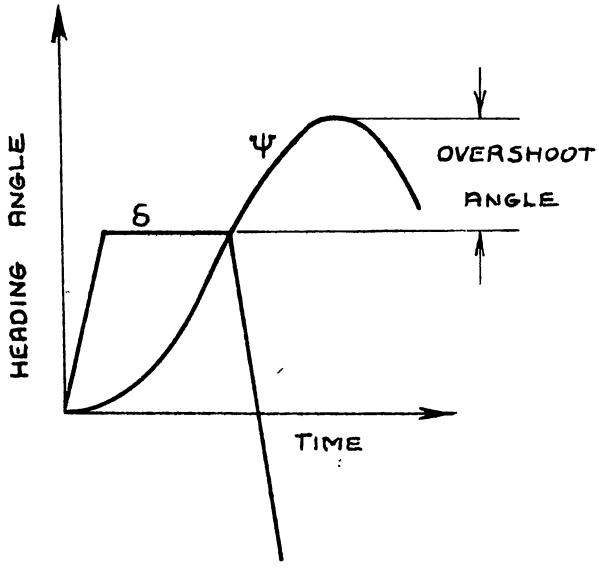

FIG. 20

CHAPTER 3

MODEL EXPERIMENTS

3.1 Set-Up of the Instrumentation

A forced yawing technique was employed in this project, and a yawing oscillator and a dynamometer were designed and constructed at The University of Michigan machine shop for this purpose. In the forced yawing technique, an oscillator yaws the model about the vertical axis through its center of gravity while the model is towed on a straight course at a constant speed. The side force and the moment applied to the model by the oscillator are measured during this test.

A schematic of the set-up of the oscillator and the dynamometer is shown in Fig. 20.a, and a photo of the whole arrangement is shown in Fig. 20.b. As seen in Fig. 20.a, a vertical shaft F is attached vertically to the towing carriage and is oscillated by a driving motor A through an arm D and a connecting rod C. The amplitude of yaw is adjusted by the eccentricity at the disc B. To the shaft F, an arm G is fixed, and two thin aluminum pipes H and I are attached to the arm through slide bearings so the model is allowed to heave and trim. Pipes H and I are fixed to the model through pivots L and M to allow the model to roll and pitch.

To the rods H and I, three sets of wire strain gauges are attached from which the drag, the side force and the yawing moment applied to the model can be measured. The amplitude of

yaw is adjustable from zero to ten degrees and the frequency of yaw is adjustable from zero to one per second; and the maximum angular velocity attained is comparable to that of the full scale ship turning with 40 degrees rudder angle.

The forces and the moment picked up by the wire strain gauges are recorded by Sanborn recorders together with the motion of the model and time signals. Examples of two sets of records are shown in Fig. 21; the upper one shows static test data with two degrees drift angle, and the lower shows oscillating test data with four degrees amplitude and 17 seconds period. Owing to practical reasons, two side forces Y_2 and Y_1, one at the C.G. of the model and one at 1.25 feet forward of the C.G. are measured instead of measuring the side force and the yawing moment. Therefore, the yawing moment is obtained as: $N=1.25Y_1$

and the total side force is: $Y=Y_1+Y_2$

Detailed procedure for obtained stability derivatives is shown in Appendix 2.

3.2 Description of the Model

A 1/64 scale wooden model of S.S. BENJAMIN FAIRLESS was used. The model is self propelled and the rudder angle can be controlled from the towing carriage. Dimensions of the model are as shown in Table 3.

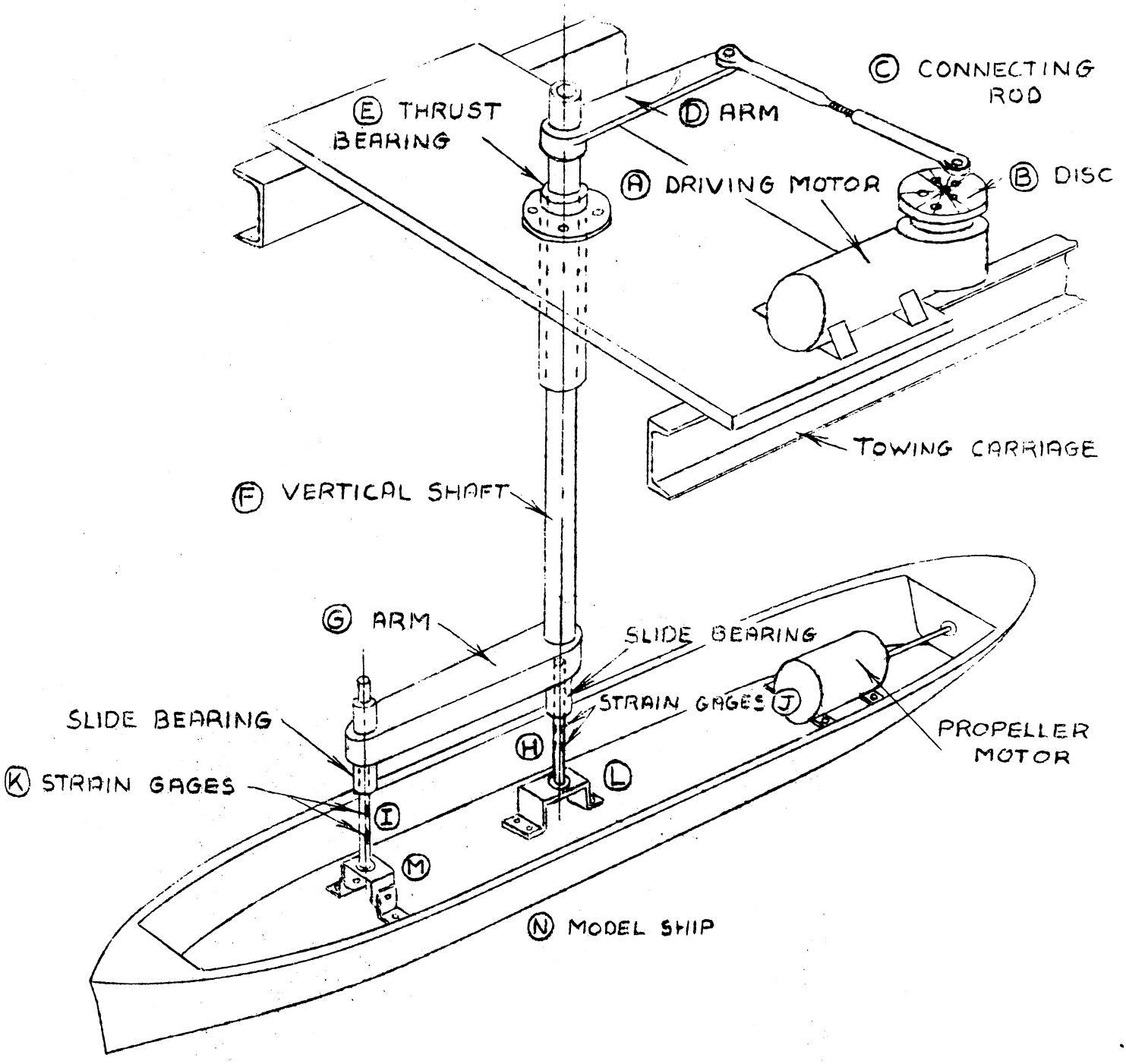

FIG. 20-a SET-UP OF SHIP MODEL OSCILLATOR AND DYNAMOMETER

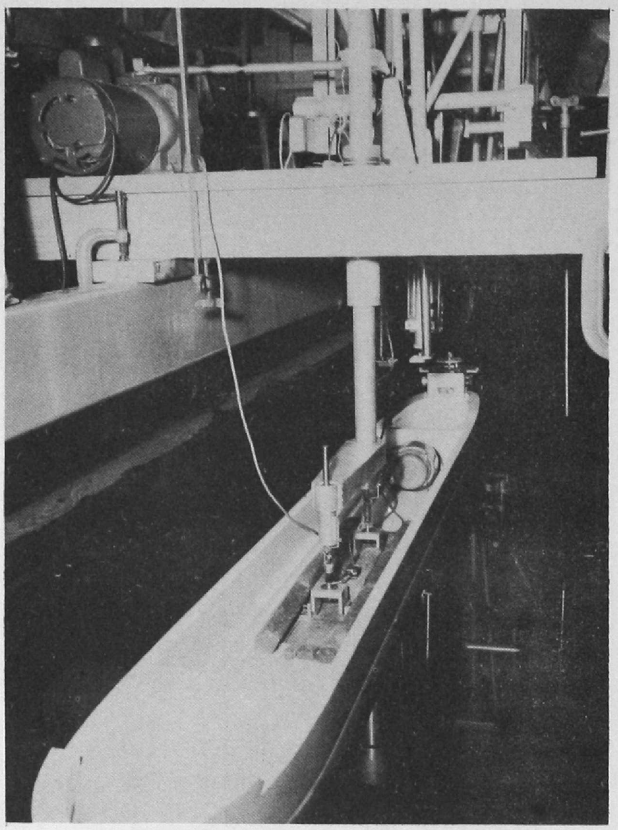

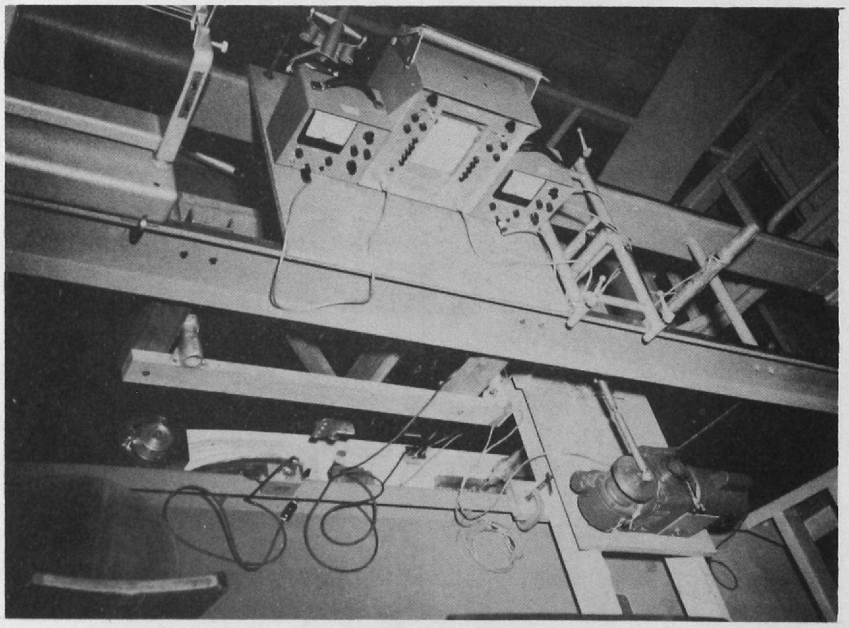

FIG. 20.b. PICTURES OF THE SET-UP OF THE INSTRUMENTATION

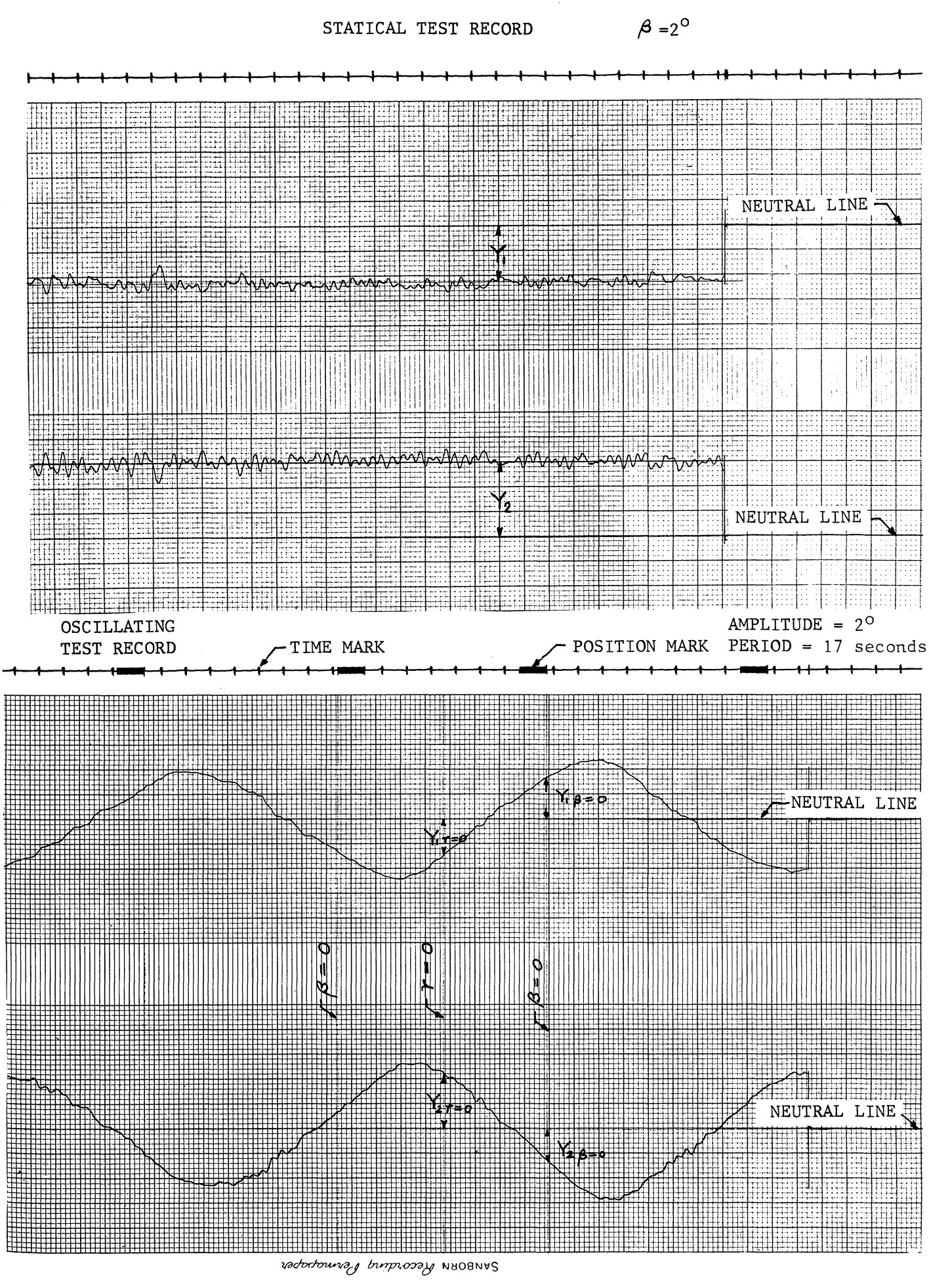

FIG. 21 EXAMPLES OF THE RECORDS

TABLE 3

MODEL DIMENSIONS

LOA	9'-11.93"	Trim Aft	0.313"
LBP	9'-8.77" 296.6 cm	Radius of gyration	1/4.32 of the ship length
D	1'-0.563"		
d (tested)	4.125" ← 85,124 kg Aspect ratio = 0.07065		
	4.5" ← 92.862 kg		

3.3 Results of Model Experiments

The yawing oscillator was completed in May 1961 and the model experiments have been conducted since then.

Tests were carried out at the same draft as full scale tests, and the speed of the model was chosen as 2.00 feet per second (60.95 cm/sec) which corresponds to 10.8 MPH in the full scale ship. Effects of change of speed and change of yawing frequency were also examined.

3.3.1 Static tests.

The side force and the yawing moment were measured while the model was towed on a straight course with specified angle of yaw (drift angle) with and without propeller working and also with various rudder angles.

Fig. 22 shows the results of tests in deep water. In this figure the side force coefficient $Y'(\beta)$ and the yawing moment coefficient $N'(\beta)$ are plotted versus the drift angle. The slopes of the tangents of $Y'(\beta)$ and $N'(\beta)$ curves at the origin give the stability derivatives;

$$Y'_\beta = \frac{\partial Y'}{\partial \beta'} \qquad N'_\beta = \frac{\partial N'}{\partial \beta'}$$

thence we get; $Y'_\beta = 7.35 \times 10^{-3}$, $N'_\beta = 2.31 \times 10^{-3}$

Rudder force and moment coefficient $Y'(\delta)$ and $N'(\delta)$ can be also obtained from $Y'(\delta)$ and $N'(\delta)$ curve versus rudder angle, and we get; $Y'_\delta = -1.69 \times 10^{-3}$, $N'_\delta = +0.813 \times 10^{-3}$/rad.

Similar tests were carried out in shallow water where the depth of water was 1.36 times of the ship's draft. The results are shown in Fig. 23 together with the deep water data. The stability derivatives are also obtained from Fig. 23 as follows;

$$Y'_\beta = 15.95 \times 10^{-3}, \quad N'_\beta = 9.58 \times 10^{-3}$$

$$Y'_\delta = -3.16 \times 10^{-3}, \quad N'_\delta = 1.019 \times 10^{-3}$$

A remarkable difference will be noticed when these figures are compared with those for deep water.

3.3.2 Oscillating tests

From the oscillating tests, the side force and the yawing moment caused by turning of the model are obtained. The effects of changes in the frequency of oscillation are checked by testing with different combinations of the frequency and the amplitude of oscillation; and it was ascertained from these tests that if the frequency of yaw is lower than 1/13, or in other words, the period of oscillation is longer than 13 seconds, then the effect of the frequency of measured values is practically negligible. Since measurement of force and moment becomes more difficult when the period of oscillation becomes longer, a period of 13 seconds is used as a standard period.

The results of the tests in deep water are given in Fig. 24

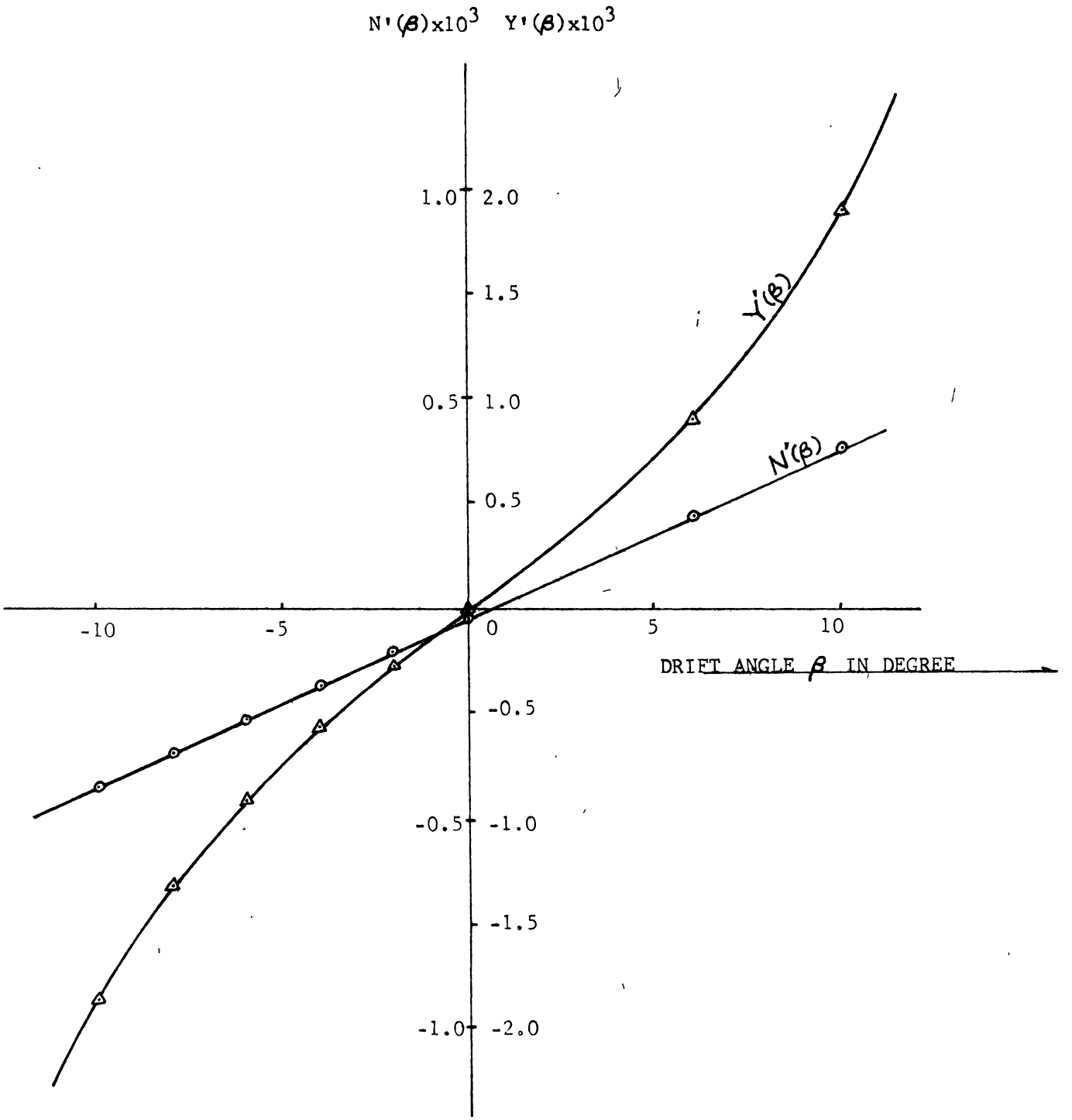

FIG. 22 SIDE FORCE AND YAWING MOMENT COEFFICIENT VERSUS DRIFT ANGLE
(IN DEEP WATER)

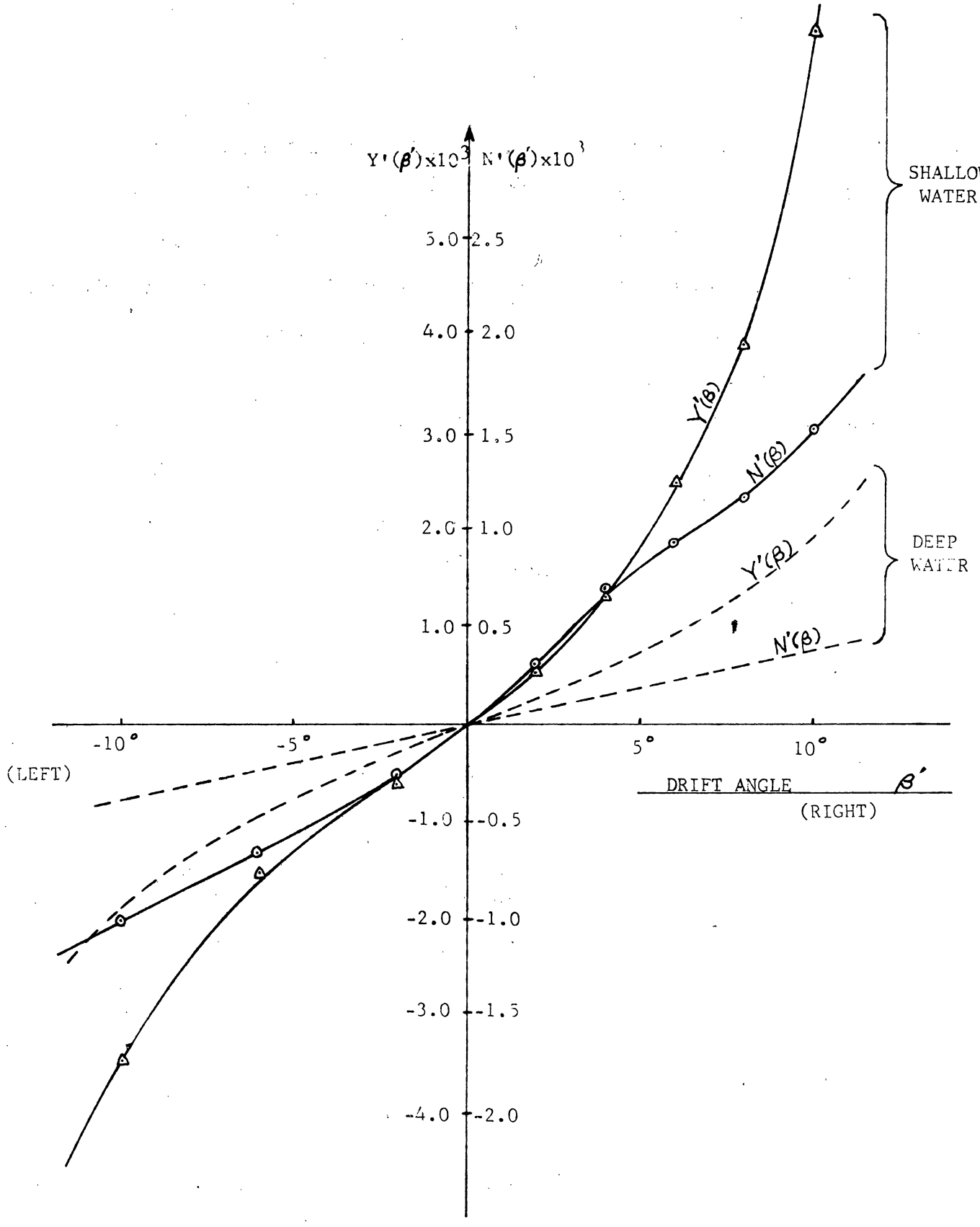

FIG. 23 SIDE FORCE AND YAWING MOMENT COEFFICIENT VERSUS DRIFT ANGLE
(IN SHALLOW WATER)

where side force coefficient $Y'(r')$ in the form of $-m'r' + Y'(r')$ and the yawing moment coefficient $N'(r')$ are plotted versus turning rate r'. Both N' and $-m'r' + Y'$ in Fig. 24 show a fairly remarkable trend toward non-linearity. From Fig. 24 we can obtain N'_r and $-m'+Y'_r$ as the slopes of the tangents to N' curve and $-m'r'+Y'$ curve at the origin.

Thence we get; $-m' + Y'_r = -5.33 \times 10^{-3}$

$N'_r = -0.877 \times 10^{-3}$

Similar tests were carried out in shallow water and results are shown in Fig. 25 together with the deep water data. Stability derivatives are also obtained from Fig. 25 as follows;

$-m' + Y'_r = -8.21 \times 10^{-3}$

$N'_r = -3.44 \times 10^{-3}$

CHAPTER 4

COMPARISON OF FULL SCALE AND MODEL DATA

To evaluate the accuracy and reliability of the model experiment data, comparison with the full scale data was made from various viewpoints.

4.1 Stability Criterion

As shown in formula (A-15) of Appendix 1, a discriminant to show whether a ship is dynamically stable or unstable on straight course is given as follows:

For stable ship $q_3 = N'_\beta (-m' + Y'_r) - Y'_\beta N'_r > 0$

For unstable ship $q_3 =$ " < 0

Using the stability derivatives obtained from the model experiments, we get;

In deep water $q_3 = -5.93 \times 10^{-6} < 0$

In shallow water $q_3 = -2.39 \times 10^{-5} < 0$

This result means that the ship is directionally unstable in both deep and shallow water. The degree of instability depends on the absolute value of the real part of equation (A-13) of Appendix 1, and is calculated to be as follows;

In deep water $1/T_1' = 0.506$

In shallow water $1/T_2' = 0.217$

From these results we can see that the ship is less unstable in shallow water than in deep water. This agrees with the full scale spiral test results (Fig. 8 and Fig. 13).

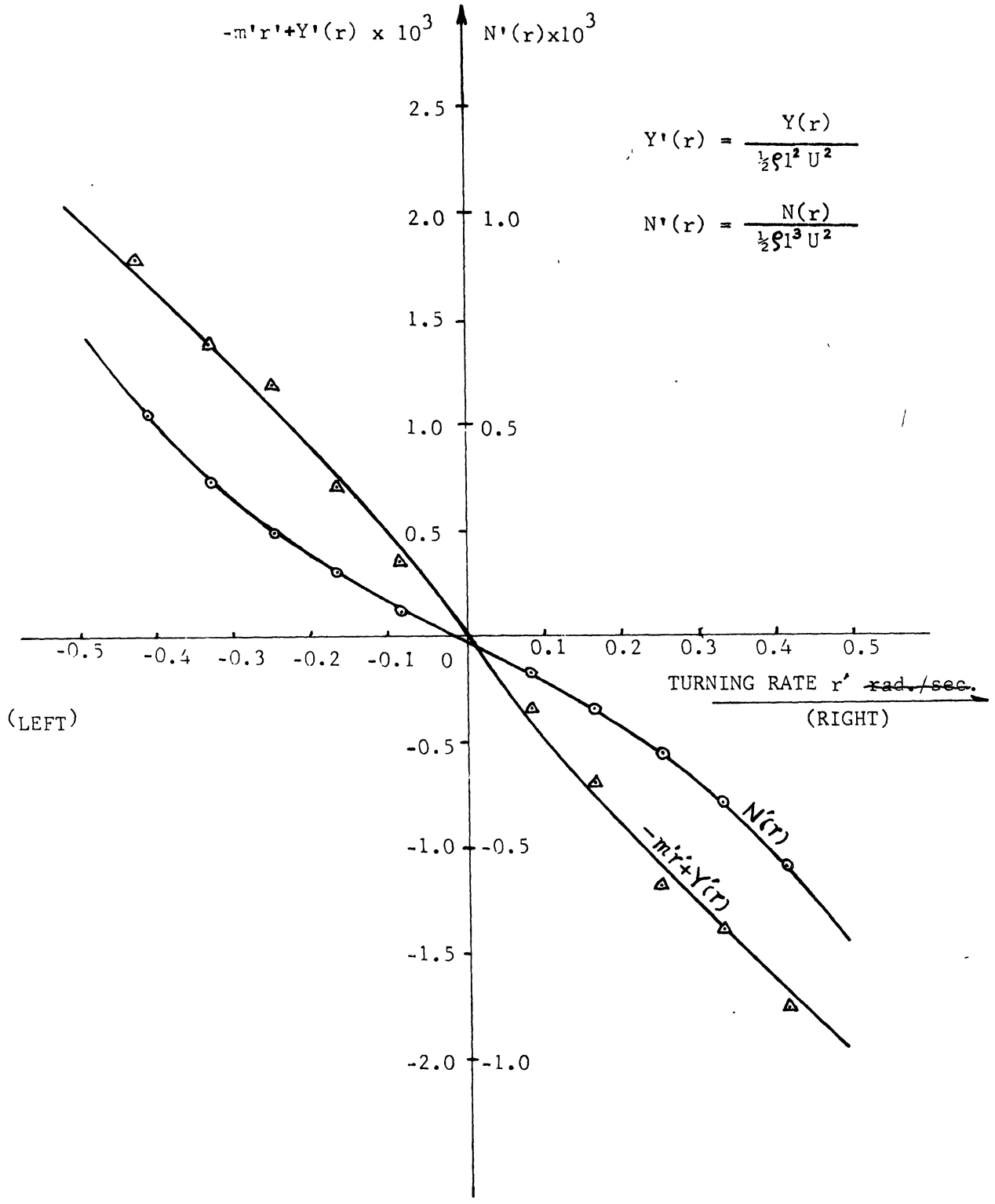

FIG. 24 SIDE FORCE AND YAWING MOMENT COEFFICIENT VERSUS TURNING RATE. (IN DEEP WATER)

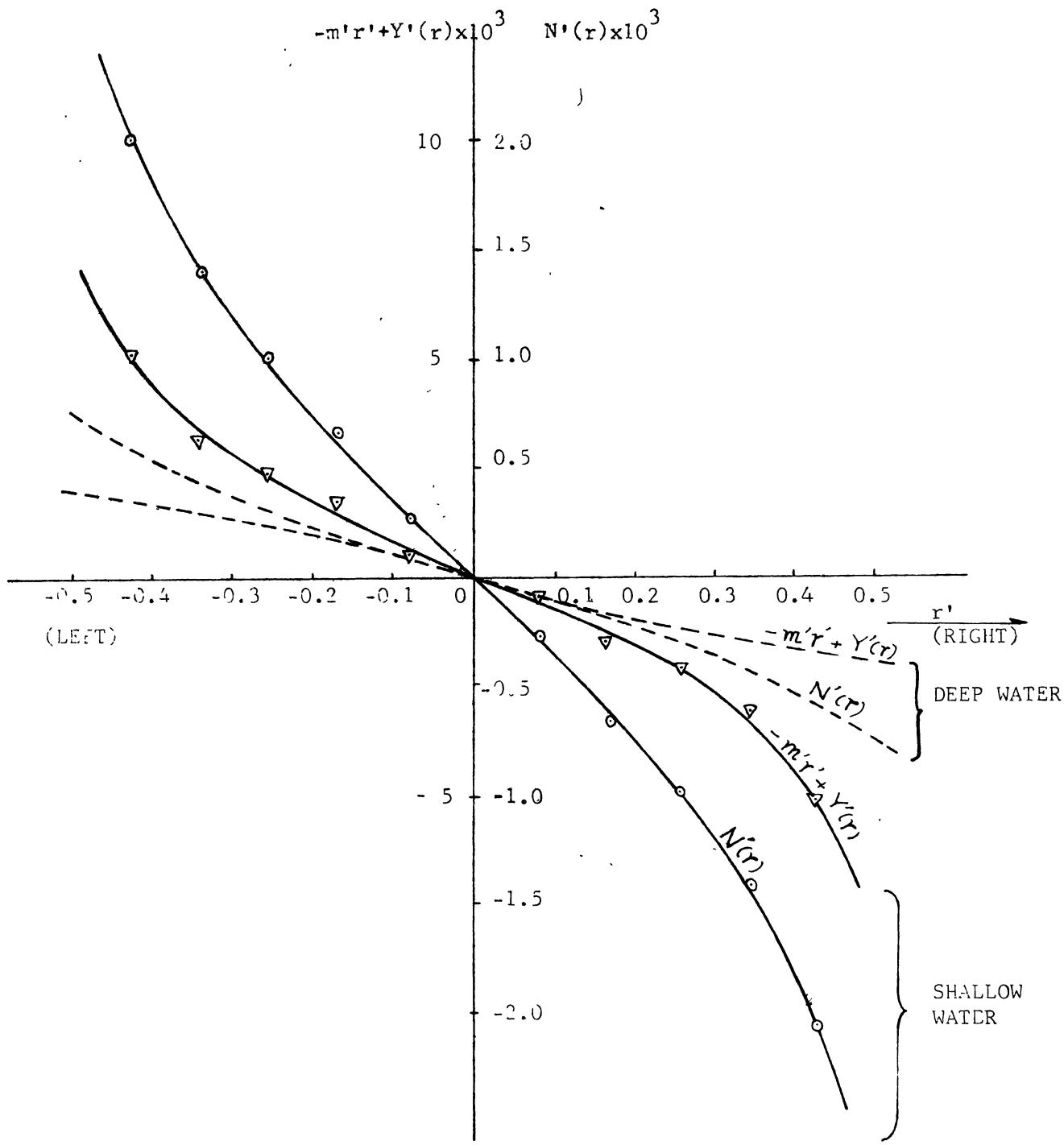

FIG. 25 SIDE FORCE COEFFICIENT AND YAWING MOMENT COEFFICIENT VERSUS ANGULAR VELOCITY (SHALLOW WATER)

4.2 Slope of the r- δ Curve at the Origin

The slope of turning rate versus rudder angle curve is one of the measures of the directional stability of ships. As the tested ship is directionally unstable, the slope is negative; therefore, it is impossible to obtain the slope from the full scale tests. But from Figs. 8 and 13, we can estimate the tangent at the origin.

On the other hand, the slope of the r- δ curve is easily calculated as shown in Appendix 1 using stability derivatives obtained by model experiments. Results of calculation are shown in Table 4 with the comparison of estimated full scale data.

TABLE 4

	Full Scale	Model
Deep Water	0.042 deg/sec/deg.	0.0433 deg/sec/deg.
Shallow Water	0.05 "	0.0547 "

Results of calculation based on the model experiment data show good agreement with full scale data.

4.3 Rate of Change of Heading versus Rudder Angle (r- δ Diagram)

From model experiment data we can calculate the approximate stationary turning rate for any specified rudder angle. Detail of procedure of the calculation is given in Appendix 3.

Results are shown in Figs. 26 and 27 together with the full scale spiral tests data. From Figs. 26 and 27 we see that the calculated curves show fairly good agreement with the full scale

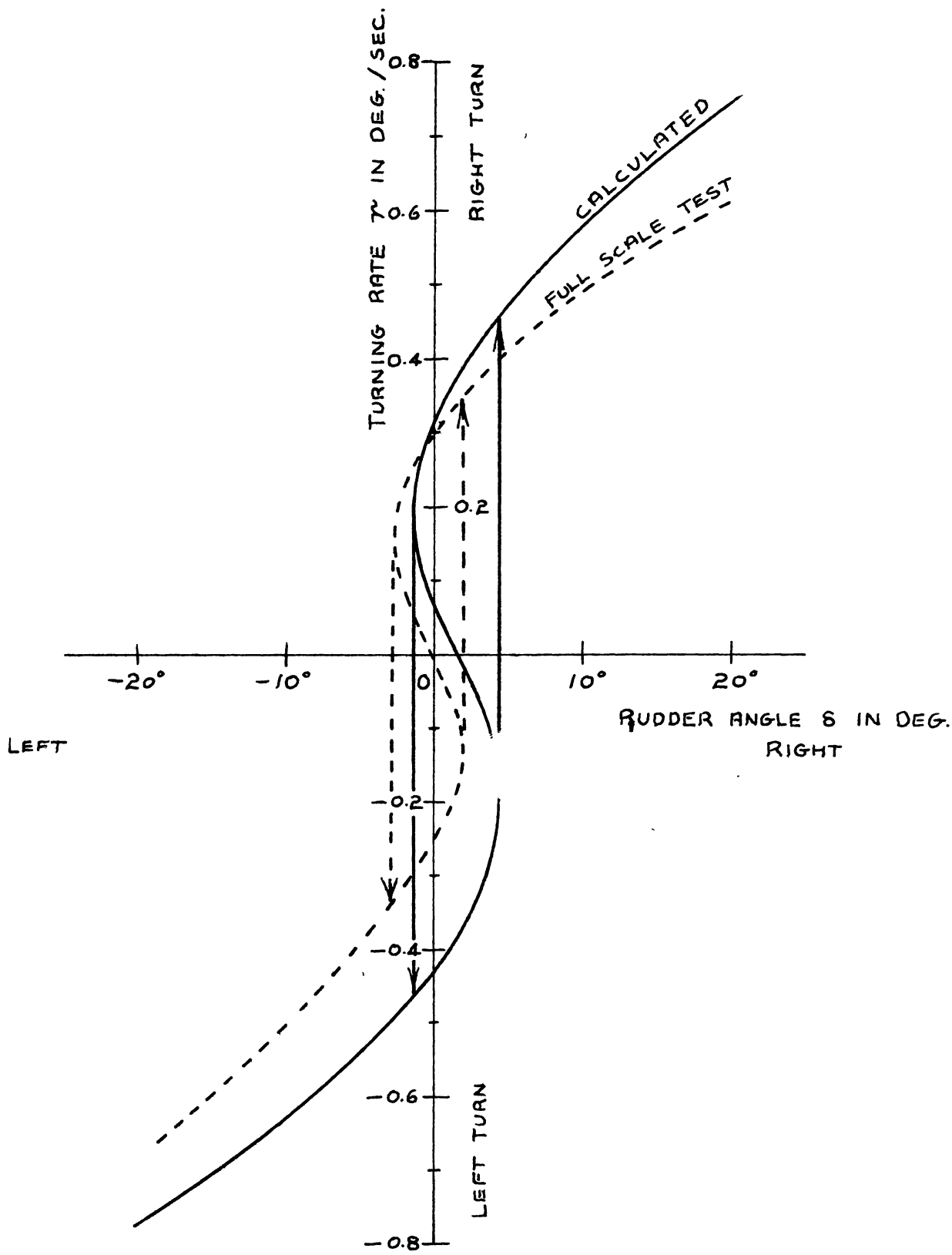

FIG. 26 TURNING RATE VS. RUDDER ANGLE (DEEP WATER)

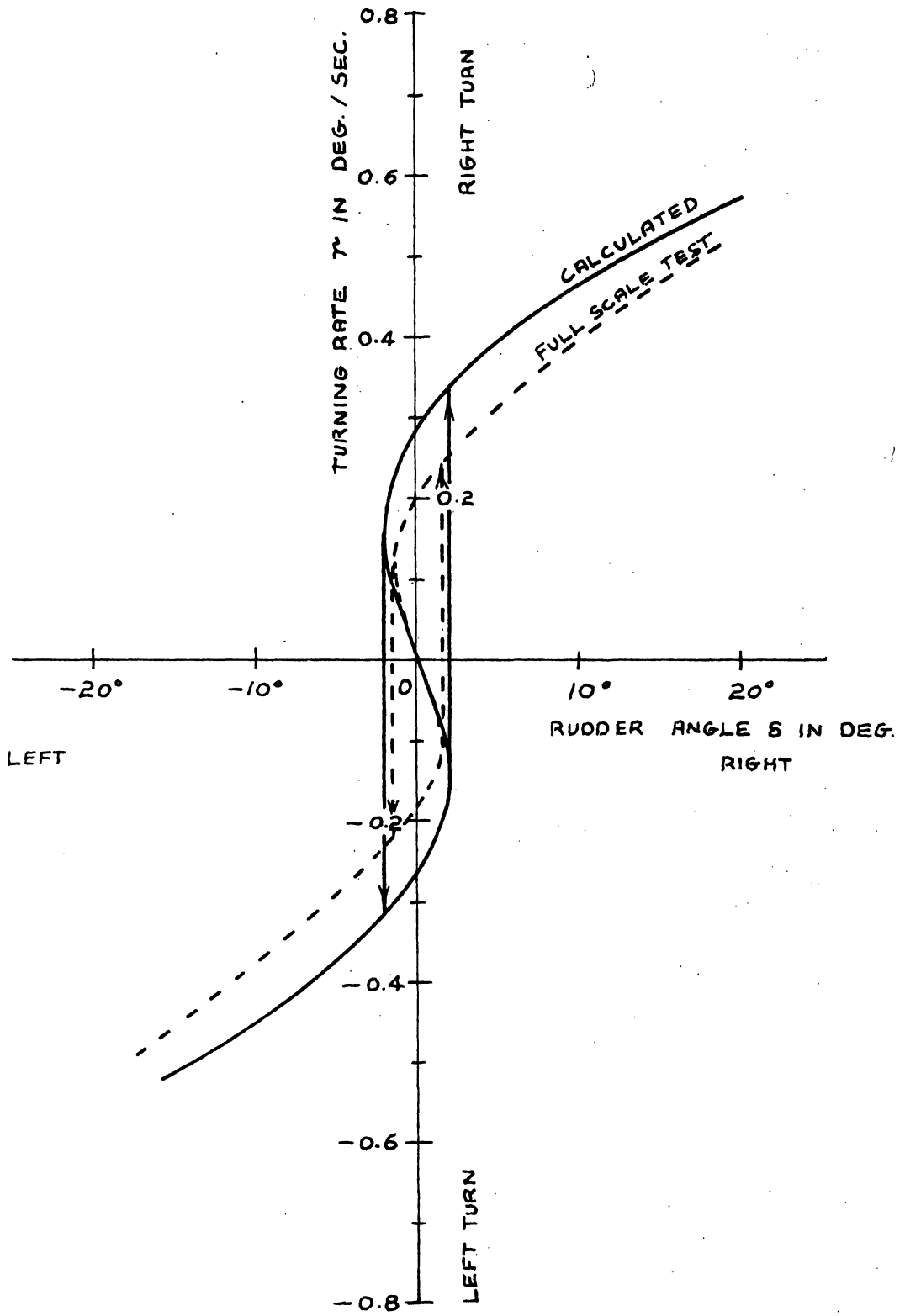

FIG. 27 TURNING RATE VS. RUDDER ANGLE (SHALLOW WATER)

data in a quantitative sense. Qualitatively, the calculated values are always larger than the full scale data, especially at large rudder angle. This deviation is believed to be mainly caused by elimination of higher order terms in the equation of motion.

To compare the calculated values with the full scale data numerically, the height and width of the hysteresis loop and the turning rate at 10° rudder angle are calculated and shown in Table 5.

TABLE 5

		Shallow Water	Deep Water	Ratio Shallow Water/ Deep Water
Height of the Loop	Full scale test	0.39 deg/sec	0.55	0.71
	Model experiment	0.54	0.74	0.73
Width of the Loop	Full scale test	3 deg.	5.0	0.60
	Model experiment	4.0	6.5	0.615
Turning Rate at 10°	Full scale test	0.39 deg/sec	0.50	0.78
	Model experiment	0.45	0.6	0.75

From Table 5, it is seen that calculated values are always larger than full scale data; however, the ratios of shallow water data to deep water data show good agreement between calculated and full scale data.

Summarizing the results of Chapter 4, it can be said that the model experiment data are in quite good agreement with full scale trial data for motions of small deviation from a straight course. Results given in 4.1 and 4.2 show this. For the motion of large deviation from a straight course, the turning rates derived from the model experiment data are always larger than the

full scale data; but as far as the percentage increase or decrease of the maneuvering quality due to restricted water effect is concerned, it appears that model experiment data may be used with satisfactory accuracy.

ACKNOWLEDGEMENTS

The following organizations were most cooperative and helpful in providing the ship and in furnishing funds for the research.

Pittsburgh Steamship Division of United States Steel Corporation

The Society of Naval Architects and Marine Engineers

The University of Michigan

The authors would also like to acknowledge the cooperation of the following individuals in advising and helping in the experiments and in editing this paper.

Members of the H-10 panel of the Society of Naval Architects and Marine Engineers.

Prof. Harry Benford

Prof. F. C. Michelsen

Capt. V. Osier

Staff members of the Ship Hydrodynamics Laboratory of The University of Michigan

Mr. N. Salvesen (student)

Mr. W. L. Scranton, III (student)

Mr. A. O. Gürkan (student)

Miss Helen Walker

REFERENCES

1 Deudonné, J.: Collected French Papers on the Route of Ships at Sea. DTMB Translation 246, Jan. 1953.

2 Tani, H.: On the Steady Turning of Directionally Unstable Ships on Straight Course. Transactions of ZOSEN KYOKAI, 1960.

3 Kempf, G.: Maneuvering Standards of Ships. Deutsche Schiffahrts Zeitschrift HANSA, No. 27/28, (1944).

4 Nomoto, K.: Analysis of Kempf's Standard Maneuver Test and Proposed Steering Quality Indices. DTMB Report 1461, 1960.

5 Gertler, M. and Gover, S. C.: Handling Quality Criteria: Chesapeake Section of the Society of Naval Architects and Marine Engineers, 1959.

6 Strandhagen, A. G.: Concept of Loop and Its Relation to Manual and Automatic Steering of Directionally Unstable Ships. Presented before the Twelfth General Meeting of the AMERICAN TOWING TANK CONFERENCE, 1959.

7 Poster, D. and Abkowitz, M. A.: Hydrodynamic Stability Derivatives and Their Use. U.S. Naval Underwater Ordnance Station TM No. 117.

8 Motora, S.: On the Course Stability of Ships. Transactions of ZOSEN KYOKAI, 1949.

APPENDIX 1

EQUATION OF MOTION AND STABILITY DISCRIMINANT

A.1.1 Equation of Motion

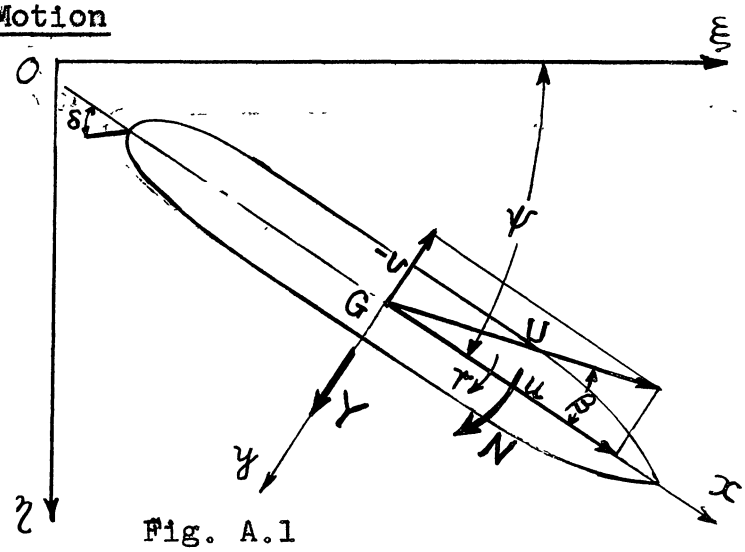

Fig. A.1

The co-ordinate is chosen as Fig. A.1 viz.; the origin is taken at the C.G. of the ship, and x and y axes are taken to be longitudinal and transverse axes of the ship. Ship's heading angle ψ is measured from a space fixed axis $O\xi$.

Then the equation of motion is written as follows;

$$\left.\begin{aligned} m\dot{v} + mur &= Y(\dot{v},\dot{r},v,r,\dot{\delta},\delta) \\ I_z\dot{r} &= N(\dot{v},\dot{r},v,r,\dot{\delta},\delta) \end{aligned}\right\} \quad (A.1)$$

Y and N can be expanded as a linear function of $\dot{v},\dot{r},v,r,\dot{\delta}$ and δ.

$$\left.\begin{aligned} Y &= Y_{\dot{v}}\dot{v} + Y_{\dot{r}}\dot{r} + Y_v v + Y_r r + Y_{\dot{\delta}}\dot{\delta} + Y_\delta \delta \\ N &= N_{\dot{v}}\dot{v} + N_{\dot{r}}\dot{r} + N_v v + N_r r + N_{\dot{\delta}}\dot{\delta} + N_\delta \delta \end{aligned}\right\} \quad (A.2)$$

Substituting (A.2) into (A.1) we get;

$$\left.\begin{aligned} (m-Y_{\dot{v}})\dot{v} - Y_{\dot{r}}\dot{r} &= Y_v v + (-mu+Y_r)r + Y_{\dot{\delta}}\dot{\delta} + Y_\delta\delta \\ (I_z-N_{\dot{r}})\dot{r} - N_{\dot{v}}\dot{v} &= N_v v + N_r r + N_{\dot{\delta}}\dot{\delta} + N_\delta\delta \end{aligned}\right\} \quad (A.3)$$

On the other hand, the equation of motion in an ideal fluid is

given as follows (7), (8):

$$\left.\begin{aligned}(m + m_y)\dot{v} + m_y\alpha\dot{r} &= -(m + m_x)ur + Y\\ (I_z+J_z)\dot{r} + m_y\alpha\dot{v} &= (m_x - m_y)uv + N\end{aligned}\right\} \qquad (A.4)$$

where α is distance between the C.G. of the ship to the center of transverse added mass m_y. Since the effect of viscosity on the added mass is very small, we cannassume the acceleration terms of the eq. (A.4) are the same; therefore we get:

$$\left.\begin{aligned}-Y_{\dot{v}} &= m_y\\ -N_{\dot{r}} &= J_z\end{aligned}\right\} \qquad \left.\begin{aligned}-Y_{\dot{r}} &= m_y\alpha = -Y_{\dot{v}}\alpha\\ -N_{\dot{v}} &= m_y\alpha = -Y_{\dot{v}}\alpha\end{aligned}\right\} \qquad (A.5)$$

Moreover, letting $N_v v$ of (A.3) includes $(m_x-m_y)uv$ of (A.4), and $Y_r r$ of (A.3) includes $-m_x ur$ of (A.3), we get:

$$\left.\begin{aligned}(m - Y_{\dot{v}})\dot{v} - Y_{\dot{v}}\alpha\dot{r} &= (-mu + Y_r)r + Y_v v + Y_{\dot{\delta}}\dot{\delta} + Y_\delta\delta\\ (I_z - N_{\dot{r}})\dot{r} - Y_{\dot{v}}\alpha\dot{v} &= N_r r + N_v\dot{v} + N_{\dot{\delta}}\dot{\delta} + N_\delta\delta\end{aligned}\right\} (A.6)$$

It is verified that if the origin is taken at the point which is the center of gravity of ship's mass m and the transverse added mass m_y $(-Y_{\dot{v}})$, the coupling terms in eq. (A.6) will disappear. This point is supposed to be very close to the C.G. of the ship since the center of m_y is generally very close to the C.G.. Therefore, we may be able to neglect $Y_{\dot{v}}\alpha\dot{r}$ and $Y_{\dot{v}}\alpha\dot{v}$ without unreasonable error.

Thus we get:

$$\left.\begin{aligned}(m-Y_{\dot{v}})\dot{v} &= (-mu + Y_r)r + Y_v v + Y_{\dot{\delta}}\dot{\delta} + Y_\delta\delta\\ (I_z - N_{\dot{r}})\dot{r} &= N_r r + N_v v + N_{\dot{\delta}}\dot{\delta} + N_\delta\delta\end{aligned}\right\} (A.7)$$

Since $v = -U\beta$, $\dot{v} = -U\dot{\beta}$ and $\dot{u} = U$ for small deviation from a straight course, we can convert the variable from v to β.

$$\left.\begin{aligned}-(m - Y_{\dot{v}})U\dot{\beta} &= (-mU + Y_r)r + Y_\beta\beta + Y_{\dot{\delta}}\dot{\delta} + Y_\delta\delta\\ (I_z - N_{\dot{r}})\dot{r} &= N_r r + N_\beta\beta + N_{\dot{\delta}}\dot{\delta} + N_\delta\delta\end{aligned}\right\} (A.8)$$

Moreover, (A.7) can be normalized by using the following non-dimensional variables.

$$\left.\begin{aligned} t' &= t\frac{U}{\ell} \\ \psi' &= \psi \qquad \beta' = \beta \qquad \delta' = \delta \\ \dot{\psi}' &= r' = r\frac{\ell}{U} \qquad \dot{\beta}' = \dot{\beta}\frac{\ell}{U} \qquad \dot{\delta}' = \dot{\delta}\frac{\ell}{U} \\ \dot{r}' &= \dot{r}\left(\frac{\ell}{U}\right)^2 \end{aligned}\right\} \quad (A\cdot 9)$$

Then (A.7) becomes:

$$\left.\begin{aligned} -(m' - Y_{\dot{v}})\dot{\beta}' &= (-m' + Y_r')r' + Y_\beta'\beta' + Y_{\dot{\delta}}'\dot{\delta}' + Y_\delta'\delta' \\ (I_z' - N_{\dot{r}}')\dot{r}' &= N_{\dot{r}}'r' + N_\beta'\beta' + N_{\dot{\delta}}'\dot{\delta}' + N_\delta'\delta' \end{aligned}\right\} \quad (A\cdot 10)$$

where

$$\left.\begin{aligned} m' &= \frac{m}{\frac{1}{2}\rho\ell^3} & I_z' &= \frac{I_z}{\frac{1}{2}\rho\ell^5} \\ Y_{\dot{v}}' &= \frac{Y_{\dot{v}}}{\frac{1}{2}\rho\ell^3} & N_{\dot{r}}' &= \frac{N_{\dot{r}}}{\frac{1}{2}\rho\ell^5} \\ Y_r' &= \frac{Y_r}{\frac{1}{2}\rho\ell^3 U} & N_r' &= \frac{N_r}{\frac{1}{2}\rho\ell^4 U} \\ Y_\beta' &= \frac{Y_\beta}{\frac{1}{2}\rho\ell^2 U^2} & N_\beta' &= \frac{N_\beta}{\frac{1}{2}\rho\ell^3 U^2} \\ Y_{\dot{\delta}}' &= \frac{Y_{\dot{\delta}}}{\frac{1}{2}\rho\ell^3 U} & N_{\dot{\delta}}' &= \frac{N_{\dot{\delta}}}{\frac{1}{2}\rho\ell^4 U} \\ Y_\delta' &= \frac{Y_\delta}{\frac{1}{2}\rho\ell^2 U^2} & N_\delta' &= \frac{N_\delta}{\frac{1}{2}\rho\ell^3 U^2} \end{aligned}\right\} \quad (A\ 11)$$

A.1.2 Stability Discriminant

Putting $\dot{\delta} = \delta = 0$ in the eq. (A.9), we can obtain a solution for r' when slightly deviate from a straight course.

$$r' = A_1 e^{-\frac{t'}{T_1'}} + A_2 e^{-\frac{t'}{T_2'}} \qquad (A\cdot12)$$

$$\left.\begin{matrix} -\frac{1}{T_1'} \\ -\frac{1}{T_2'} \end{matrix}\right\} = -\frac{q_2}{2q_1} \begin{pmatrix} + \\ - \end{pmatrix} \frac{\sqrt{q_2^2 - 4q_1q_3}}{2q_1} \qquad (A\cdot13)$$

where :

$$\left.\begin{aligned} q_1 &= (m' - Y_{\dot{v}}')(I_z' - N_{\dot{r}}') \\ q_2 &= Y_\beta'(I_z' - N_{\dot{r}}') - (m' - Y_{\dot{v}}')N_{\dot{r}}' \\ q_3 &= N_\beta'(-m' + Y_{r'}') - Y_\beta' N_{r'} \end{aligned}\right\} \qquad (A\cdot14)$$

Since q_1 and q_2 are always positive, the sign of $1/T_1'$ and $1/T_2'$ are determined by the sign of q_3; therefore,

if:		
$q_3 > 0$,	$-1/T_1' < 0$	directionally stable
$q_3 < 0$,	$-1/T_1' > 0$	directionally unstable

(A.15)

A.1.3 Relationship Between Slope of r-δ Diagram at the Origin and the Directional Stability

Ship's steady rate of change of heading r, for specified rudder angle will be obtained from the eq. (A.10) putting accelerations $\dot{\beta}$ and $\dot{r}$ to be zero.

Therefore we get:

$$r = \frac{Y_\beta' N_\delta' - Y_\delta' N_\beta'}{q_3} \cdot \delta \qquad (A\cdot16)$$

Slope of this diagram at $\delta = 0$ is:

$$\left(\frac{\partial r}{\partial \delta}\right)_{at\ \delta=0} = \frac{Y_\beta' N_\delta' - Y_\delta' N_\beta'}{q_3} \qquad (A\cdot17)$$

Since the denominator of the eq. (A.17) is the same as the discriminant (A.15), which decides the directional stability of a ship, and the numerator is always positive; therefore, it follows:

$\frac{\partial r}{\partial \delta}$ is positive when the ship is directionally stable.

$\frac{\partial r}{\partial \delta}$ is zero when the ship is neutral.

$\frac{\partial r}{\partial \delta}$ is negative when the ship is directionally unstable.

APPENDIX 2

ANALYSIS OF FORCED YAWING TEST DATA

The side force and moment measured by the dynamometer when the model is forced to yaw by the oscillator are obtained by the eq. (A.5) putting $Y_\delta = Y_{\dot\delta} = N_\delta = N_{\dot\delta} = 0$.

$$\left.\begin{aligned} &\text{Total side force } Y = (m - Y_{\dot v})\dot v - Y_{\dot v}\alpha\,\dot r - Y_v v + (-mu + Y_r)r \\ &\text{Total moment } \quad N = (I_Z - N_{\dot r})\dot r - Y_{\dot v}\alpha\,\dot v - N_v v - N_r r \end{aligned}\right\} \quad (A.19)$$

In this particular case, the C.G. of the model is traveling on a straight course; therefore: $\beta = \psi$, $\dot\beta = \dot\psi = r$

and hence: $-U\beta \doteq v$, $u \doteq U$,

we can rewrite (A.19) as follows:

$$\left.\begin{aligned} Y &= -(m - Y_{\dot v})Ur - Y_{\dot v}\alpha\,\dot r - Y_\beta\beta - (-mU + Y_r)r \\ N &= (I_Z - N_{\dot r})\dot r + Y_{\dot v}\alpha\,Ur - N_\beta\beta - N_r r \end{aligned}\right\} \quad (A.20)$$

Since the motion of the model is sinusoidal:

$$\beta = B\sin\omega t \qquad \ddot\beta = \dot r = -B\omega^2\sin\omega t = -\omega^2\beta$$

were ω is the circular frequency of the yawing.

Therefore we get:

$$\left.\begin{aligned} Y &= -(-Y_{\dot v}\alpha\,\omega^2 + Y_\beta)\beta - (-Y_{\dot v}U + Y_r)r \\ N &= -\{(I_Z - N_{\dot r})\omega^2 + N_\beta\}\beta - (-Y_{\dot v}\alpha U + N_r)r \end{aligned}\right\} \quad (A.21)$$

If we measure the values of Y and N at $\beta = 0$ (straight course) and at $r = 0$ (maximum deflection), and denote them as $Y_{\beta=0}$, $N_{\beta=0}$, $Y_{r=0}$, and $N_{r=0}$, we get:

$$\left.\begin{aligned} -Y_{\beta=0} &= (-Y_{\dot v}U + Y_r)r_o & -N_{\beta=0} &= (-Y_{\dot v}\alpha U + N_r)r_o \\ -Y_{r=0} &= (-Y_{\dot v}\alpha\,\omega^2 + Y_\beta)\beta_o & -N_{r=0} &= \{(I_Z - N_{\dot r})\omega^2 + N_\beta\}\beta_o \end{aligned}\right\} \quad (A.22)$$

As Y_β and N_β are obtained by statical tests, we can obtain Y_r, N_r, $Y_{\dot{v}}$, α and $I_z - N_{\dot{r}}$ from the eq. (A.22) provided either $Y_{\dot{v}}$ or α is known.

In the practical case, Y_1 and Y_2 are measured at $\beta = 0$ and at $r=0$ instead of measuring Y and N. (refer Fig. 21).

APPENDIX 3

CALCULATION OF THE RATE OF CHANGE OF COURSE VERSUS RUDDER ANGLE DIAGRAM

As shown in A.1.3, turning rate for specified rudder angle is easily calculated by eq. (A.16) using stability derivatives when the hydrodynamic forces and moments are linear. However, in actual cases, hydrodynamic forces and moments are non-linear for the motion of large deviation from a straight course; therefore such simplified calculations are not practicable.

While the hydrodynamic force Y and moment N are assumed to be linear functions of $\dot{\beta}$, $\dot{r}$, β, r, $\dot{\delta}$, and δ in eq. (A.2), we may assume as a second order approximation that Y and N are the summations of higher order functions of $\dot{\beta}, \ldots\ldots \dot{\delta}$:

$$\left.\begin{aligned} Y &= Y(\dot{\beta}) + Y(\dot{r}) + Y(\beta) + Y(r) + Y(\dot{\delta}) + Y(\delta) \\ N &= N(\dot{\beta}) + N(\dot{r}) + N(\beta) + N(r) + N(\dot{\delta}) + N(\delta) \end{aligned}\right\} \quad (A.23)$$

Therefore, eq. (A.8) can be rewritten as follows:

$$\left.\begin{aligned} -mU\dot{\beta} + Y(\dot{\beta}) &= -mUr + Y(r) + Y(\beta) + Y(\dot{\delta}) + Y(\delta) \\ I_z\dot{r} - N(\dot{r}) &= N(r) + N(\beta) + N(\dot{\delta}) + N(\delta) \end{aligned}\right\} \quad (A.24)$$

Putting accelerations $\dot{\beta}$, $\dot{r}$, and $\dot{\delta}$ to be zero, we get:

$$\left.\begin{aligned} -mUr + Y(r) + Y(\beta) + Y(\delta) &= 0 \\ N(r) + N(\beta) + N(\delta) &= 0 \end{aligned}\right\} \quad (A.25)$$

The solution of eq. (A.25) gives the steady turning rate r and corresponding drift angle β for any specified rudder angle δ. Y(r), Y(β), N(r) and N(β) are as shown in Figs. 22 through 25, and it is possible to approximate them by polinomials of r and β

as was shown by Strandhagen (6). However, in this paper, a simpler graphical method was employed to obtain the solutions and $Y(\beta),.....N(r)$ are used in their original shapes as shown in Figs. 22 through 25.

Solutions are obtained in the following manner:

(1) A certain value of r is assumed to be a solution, and the value of N(r) is read from Fig. 25.

(2) From the second eq. of (A.25), $N(\beta)$ is calculated, and corresponding β is read from Fig. 23.

(3) Using the above value of β, the corresponding value of $Y(\beta)$ is taken from Fig. 23.

(4) From the first eq. of (A.25), Y(r) is calculated, and corresponding r is obtained from Fig. 25.

This procedure is repeated until the final r coincides with the assumed r, in which case the final r satisfies eq. (A.25).

DATE DUE

FEB 26 '70			

HIGHSMITH 45-220

C-1